An Integral-Spectral Approach for Reacting Poiseuille Flows

Pedro Arce, B. R. Locke, and I. M. B. Trigatti
Dept. of Chemical Engineering, FAMU–FSU College of Engineering, Tallahassee, FL 32310

An integral-spectral formulation for laminar reacting flows in tubular geometry (tubular Poiseuille flows) is introduced and performed within an operator–theoretic framework where the original convective-diffusive differential transport problem coupled with reaction is inverted to give an integral equation. This equation is of second kind and of the Volterra type with respect to the axial coordinate of the tube with a kernel given by Green's function. Green's function is identified by a methodology that gives the Mercier spectral expansion in terms of eigenvalues and eigenfunctions of the Stürm–Liouville problem in the radial variable of the tube. Eigenvalue problems for both Dirichlet and von Neumann boundary conditions are solved in terms of analytical functions (Poiseuille functions) and compared with the values found in the literature. The groundwork is set for future applications of the methodology to solving a wide variety of problems in convective–diffusive transport and reaction. Examples with wall and bulk chemical reaction are given to illustrate the technique.

Introduction

Heat or mass transfer in cylindrical tubes or rectangular channels under laminar flow conditions coupled with homogeneous and heterogeneous sources are important in a very large range and number of technological applications of current interest. Traditional applications in heat exchangers have utilized sinusoidal wall flux variations (Hsu, 1965a; Glasstone, 1966) as in the cooling of nuclear reactors, and more modern uses may add homogeneous microwave sources for heating or drying processes (Ayappa et al., 1991). Reaction systems under laminar flow conditions have been studied in, for example, heterogeneous catalytic reactors such as monolithic converters (Young and Finlayson, 1976) and in homogeneous tubular reactors (Rothenberg and Smith, 1966; Andersen and Coull, 1970; Linn and Huff, 1971; Golding and Dussalt, 1978). A plethora of mass transfer/separation processes that function under laminar conditions have arisen since the advent of synthetic membranes. Hollow fiber ultrafiltration, liquid membranes for facilitated transport separations, and other permselective membranes may utilize laminar flow on one or both sides of the membrane. The coupling of catalytic reactions with membrane separations first arose in immobilized enzyme and cell systems where the heterogeneous (cell or enzyme) reactions occur in the pore space of the membrane bounded by fluid flowing in laminar flow (Kim and Stroeve, 1988; Kitano and Ise, 1984; Davis and Watson, 1985). The advantages of these coupled separation/reaction processes have rapidly been incorporated in nonbiochemical or biological reactors such as ceramic membranes impregnated with hydrogenation, dehydrogenation, and other petroleum catalysts (Ziaka et al., 1993), and in phase transfer catalysis in membrane reactors (Stanley and Quinn, 1987).

A very large class of laminar-flow-based (nonreactive) separation processes called field flow fractionation (FFF) has also been developed by Giddings (1991). These processes use laminar flow in a thin channel coupled with a perpendicularly applied external field (such as electrical, centrifugal, magnetic, thermal, cross-flow, and dielectric). In addition, laminar flow in tubes with radial diffusion has been analyzed beginning with Taylor (1953, 1954a,b) and continuing with Aris (1956) and Brenner (1991) to determine effective dispersion parameters.

Although many attempts have been made to obtain a general closed-form solution for laminar systems that include transport coupled with chemical reactions or other sources, these efforts have been limited to first-order reactions or lin-

Present address of I. M. B. Trigatti: Economic Research Services, Inc., Tallahassee, FL 32303.

ear sources (Schechter and Wissler, 1960) and to simple and very particular limiting cases (Nigam, 1982; Mansour et al., 1989; Barouh and Mikhailov, 1989, 1990). Furthermore, the techniques used in the past have been mostly (a) numerical approaches (Hsu, 1965b; Andersen and Coul, 1970; Solomon and Hudson, 1971; Urtigaga et al., 1992), (b) approximate methods (Tereck et al., 1987) that solve only certain aspects of the general problem, and (c) the methods of moments (Aris, 1980), which do not yield a detailed solution but rather give information about averaged quantities. The present study introduces an integral equation analysis of laminar flow systems with heat or mass transport coupled with homogeneous (bulk) and heterogeneous (wall) sources.

The integral equation methodology developed here permits a derivation of "closed"-form solutions to problems with laminar flow (with negligible axial energy or mass dispersion) for a variety of different situations. Integral equations play a very important role in determining the existence of uniqueness conditions, deriving bounds for the solutions, and for devising efficient numerical schemes (Goldberg, 1979; Jaswon and Symm, 1977; Delves and Walsh, 1974). Some problems in the area of transport and reaction have been examined with integral equations; however, these studies have focused on fairly simple situations (Gidaspow, 1971) or specific cases with certain types of reactions (Lee and Aris, 1977; Schilson and Amundson, 1961), and it seems that the power of integral equations to simplify the computational scheme has been overlooked. Arce et al. (1988), and Grau et al. (1988) used integral equations to analyze laminar flow reactors and mass transfer devices, respectively. More recently, Karrilla and Kim (1989) have reported a very detailed account of the use of integral equations in the area of fluid mechanics (see also Kim and Karrilla, 1991; and Tanzosh et al., 1992), and Stewart et al. (1991) have proposed the use of integral equations for packed-bed reactors.

In the present article, the governing integral equations are derived through the Green's function method (Weinberger, 1965) following an approach that relates the Green's function to the spectral expansion (Mercer's expansion; Courant and Hilbert, 1953) in terms of the eigenvalues and eigenvectors of the linear transport problems. These eigenvalues and eigenvectors are obtained from Poiseuille's functions (Lawerier, 1950, 1951), and this yields a computational strategy where the linear transport terms are uncoupled from the nonlinear source terms. This strategy considerably simplifies the performance of parametric studies since the eigenvalues and eigenvectors of the Stürm–Liouville problem are computed once, independently of all input and/or wall conditions. The strategy allows the exploration of a wide range of parameter values with a minimum of computation. In previous approaches (Dranoff, 1961; Lupa and Dranoff, 1966) it was necessary to recompute all the eigenvalues for each case whenever a physical parameter was varied. Problems that include mass or heat transport (with or without linear or nonlinear chemical reactions or heat sources) at the wall can be solved by the present integral–spectral (boundary) equation approach. This approach leads to a drastic reduction in grid requirements with respect to other methods such as finite differences or finite element methods. The models solved in this article include Dirichlet- and von Neumann-type boundary conditions at the wall.

The use of integral equations makes it possible to account for a number of very different physical cases using a single unified scheme. For example, a nonuniform input temperature coupled to an axial variation of heating (or cooling) at the wall can be analyzed with the same computational scheme (with minor changes) as for the case of uniform input temperature and constant wall temperature. In addition, the relative importance of the different contributions (e.g., the energy due to the input flow, the energy due to a homogeneous heat source and the energy due to the wall flux) to the temperature profile can be clearly identified. The general and integral formulation, analysis of the Stürm–Liouville problems, the general computational strategy, and selected applications to processes with chemical reactions are given in the present article.

Model Formulation

The mathematical model for the general problem is formulated in this section. It is assumed that a solution with a concentration $c^0(r)$ is fed into a cylindrical tube, at the position $z = 0$, containing a Newtonian fluid with fully developed flow with constant physical properties. A homogeneous chemical reaction with global kinetics given by $R_b(\hat{c},T)$ takes place in the bulk of the fluid, and a catalytic heterogeneous reaction with rate $R_w(z)$ occurs at the wall of the reactor. Under these assumptions, the nondimensional steady-state axially symmetric molar species continuity equation is

$$2U\left(1-\frac{r^2}{R^2}\right)\frac{\partial \hat{c}}{\partial z} = D\left[\frac{1}{r}\frac{\partial}{\partial r}\left(r\frac{\partial \hat{c}}{\partial r}\right)+\frac{\partial^2 \hat{c}}{\partial z^2}\right]+R_b(\hat{c},T). \quad (1)$$

The homogeneous rate function $R_b(\hat{c},T)$ can be any nonlinear function of the concentration and temperature variables; it is only restricted by the usual smoothness conditions required to describe the kinetics of chemical reactions. For the present analysis we will be concerned with isothermal reactors and will not account for the temperature dependence of R_b; we use the present notation in light of a forthcoming study to treat applications with simultaneous heat and mass transfer with chemical reactions. D is the diffusion coefficient of the solute in the low concentration limit (Bird et al., 1960) and U is the average velocity in the tube. Nondimensional variables can be defined as

$$\xi \equiv \frac{Dz}{UR_t^2}; \qquad \rho \equiv \frac{r}{R_t}; \qquad c \equiv \frac{\hat{c}}{c^0};$$

$$Pe_m \equiv UR_t/D \quad \hat{\Omega} \equiv \frac{R_b R_t^2}{c^0 D}; \qquad \alpha = 2PeGe, \quad (2)$$

where Pe_m is the Peclet number for mass transfer. By using these dimensionless quantities, Eq. 1 is transformed into the nondimensional differential balance

$$\alpha(1-\rho^2)\frac{\partial c}{\partial \xi} = \frac{1}{\rho}\frac{\partial}{\partial \rho}\left(\rho\frac{\partial c}{\partial \rho}\right)+\frac{1}{Pe_m^2}\frac{\partial^2 c}{\partial \xi^2}+\hat{\Omega}(c,\theta). \quad (3)$$

By assuming that Pe_m takes large values, Eq. 3 reduces to

$$\alpha R(\rho)\frac{\partial c}{\partial \xi} = \frac{\partial}{\partial \rho}\left(\rho \frac{\partial c}{\partial \rho}\right) + R(\rho)Q(c,\theta), \tag{4}$$

where $R(\rho) \equiv \rho(1-\rho^2)$ and the nondimensional reaction rate is

$$Q(c,\theta) \equiv \frac{\hat{\Omega}(c,\theta)}{(1-\rho^2)}.$$

Boundary Conditions at the Wall. Chemical tubular reactors may have one of two types of general boundary conditions at the wall of the tube. For example, when a catalytic chemical reaction takes place at the wall of the tube, the diffusive flux must match the rate of consumption (or production) by chemical reaction at the wall through

$$-D\left.\frac{\partial \hat{c}}{\partial r}\right|_{r=R_t} = R_w(\hat{c}_w, T_w), \tag{5}$$

where $R_w(\hat{c}_w, T_w)$ is a general reaction rate function. Equation 5 is a generalized von Neumann type of boundary condition. For the case of linear physical equilibrium at the wall Eq. 5 must be replaced by

$$\hat{c}(1,z) = K(T_w)c_w(z), \tag{6}$$

where $K(T_w)$ is a partition equilibrium coefficient. Equation 6 is a generalized Dirichlet boundary condition.

Other Boundary and Entrance Conditions. In order to close the differential models just discussed, symmetry conditions at the center of the tube ($r = 0$) and conditions at the entrance of the tube ($z = 0$) must be specified. The symmetry conditions are

$$\frac{\partial \hat{c}}{\partial r}(0, z=0) = 0 \qquad \forall z \in 0 < z < L \tag{7a}$$

and the inlet distribution is

$$\hat{c}(r,0) = c^0(r) \qquad \forall r \in 0 < r < R_t. \tag{7b}$$

Nondimensional Forms of the Boundary Conditions. The boundary conditions, Eqs. 5 and 7a, for the material balances can be reduced, using the nondimensional variables defined by Eq. 2, to the nondimensional equations

$$\left.\frac{\partial c}{\partial \rho}\right|_{\rho=0} = 0 \qquad \forall \xi > 0 \tag{8a}$$

$$\left.\frac{\partial c}{\partial \rho}\right|_{\rho=1} = \Omega_w(c_w, \theta_w) \qquad \forall \xi > 0 \tag{8b}$$

where

$$\Omega_w = -R_w(c_w)\frac{R}{c_0}D.$$

The boundary condition given by Eq. 7b now becomes

$$c(\rho,0) = c_e(\rho), \qquad \forall \rho \in 0 < \rho < 1, \tag{9}$$

where $c_e(\rho)$ is a dimensionless entrance condition, and that given by Eq. 6 is

$$c(1,\xi) = \beta c_w(\xi), \tag{10}$$

where β is a nondimensional equilibrium coefficient.

General Integral Formulation

The differential models formulated earlier are parabolic differential equations with nonhomogeneous terms and with boundary conditions of first (Dirichlet), or second (von Neumann) kind. In this section an operator-theoretic analysis of the differential problem will be followed to identify the Stürm-Liouville problem associated with the radial coordinate, ρ. Therefore, a differential operation L, Hilbert space, H, a domain, $D(L)$, and an inner product will be defined and systematically used to derive the integral equation associated with the parabolic differential problem. Two additional differential operations (i.e., H_ξ and $\hat{H}_\xi$) are also required. They are defined on the basis of the radial diffusion operation L and the first derivative with respect to the axial variable, ξ (i.e., $\partial(\cdot)/\partial\xi$). The approach just outlined leads to a very efficient transformation of the differential model into the integral (formal) solution of the problem. This brings considerable advantages with respect to other transformation procedures proposed previously (Arce et al., 1983, 1988; Beck et al., 1992) and also it leads to a very useful framework to be extended to other physical situations. The differential operation L is given by

$$L \equiv -\frac{1}{R(\rho)}\frac{d}{d\rho}\left(\rho\frac{d(\cdot)}{d\rho}\right) \tag{11}$$

and the domain associated with this differential operation is defined below. Let w be an element of the Hilbert space, H, then:

$$D(L) \equiv \{w \in H \text{ and } Lw \in H: \quad w_\rho(0) = 0;\ w(1) = 0\} \tag{12}$$

for a Dirichlet condition at $\rho = 1$ and

$$D(L) \equiv \{w \in H \text{ and } Lw \in H: \quad w_\rho(0) = 0;\ w_\rho(1) = 0\} \tag{13}$$

for von Neumann boundary conditions where the subscript ρ denotes differentiation with respect to ρ. H is a set of functions that are defined as

$$H \equiv \{L_2[0,1];\ R(\rho)\} \qquad \|w\| \equiv \int_0^1 R(\rho')w^2(\rho')d\rho', \tag{14}$$

where $R(\rho) = \rho(1-\rho^2)$ and $w \equiv \{w(\rho)\}$ represents functions in the vector space H. Now the inner product in H is defined as

$$\langle w_1, w_2 \rangle \equiv \int_0^1 d\rho' R(\rho') w_1(\rho') w_2(\rho') < \infty. \qquad (15)$$

The formal solution to the general problems under consideration here may be obtained in terms of the Green's function of the parabolic differential operations associated with the differential problems. Using Eqs. 4 and 11 a parabolic differential operation H_ξ can be defined as

$$H_\xi c \equiv \left[\alpha \frac{\partial(\cdot)}{\partial \xi} + L \right] c = Q(\boldsymbol{x}, c), \qquad (16)$$

where the subscript ξ indicates the explicit use of the derivative with respect to the axial variable. Introducing a test function $G(\boldsymbol{x};\boldsymbol{x}')$ applying the inner product given by Eq. 15 and integrating Eq. 16 from $\xi = 0$ to $\xi + \epsilon$ gives

$$\int_0^{\xi+\epsilon} d\xi' \langle G(\boldsymbol{x};\boldsymbol{x}'), H_\xi c(\boldsymbol{x}') \rangle = \int_0^{\xi+\epsilon} d\xi' \langle G(\boldsymbol{x};\boldsymbol{x}'), Q(\boldsymbol{x}') \rangle. \qquad (17)$$

Successive integration by parts leads to

$$\begin{aligned} &\int_0^{\xi+\epsilon} d\xi' \langle \hat{H}_\xi G(\boldsymbol{x};\boldsymbol{x}'), c(\boldsymbol{x};\boldsymbol{x}') \rangle \\ &\quad - \int_0^{\xi+\epsilon} d\xi' [G(x;1,\xi') c_\rho(1,\xi') - G_\rho(\boldsymbol{x};1,\xi') c(1,\xi')] \\ &\quad + \alpha \int_0^1 d\rho' R(\rho') [c(\rho', \xi+\epsilon) G(\boldsymbol{x};\rho', \xi+\epsilon) \\ &\quad - c(\rho', 0) G(\boldsymbol{x};\rho', 0)] \\ &\quad = \int_0^{\xi+\epsilon} d\xi' \langle G(\boldsymbol{x};\boldsymbol{x}'), Q(x') \rangle, \end{aligned} \qquad (18)$$

where the subscript ρ in $G_\rho(\cdot)$, $c_\rho(\cdot)$ indicates differentiation with respect to the radial variable, ρ and $\hat{H}_\xi \equiv -\alpha(\partial(\cdot)/\partial\xi) + L$. The operator $\hat{H}_\xi$ is the adjoint operator of the parabolic differential operator H_ξ defined previously (Haberman, 1987). Equation 18 is a general result that holds for both cases of von Neumann and Dirichlet boundary conditions at the wall. In order to obtain the formal solutions from Eq. 18, it is useful to define the following problem for the test function $G(\boldsymbol{x};\boldsymbol{x}')$ (Weinberger, 1965; Haberman, 1987)

$$\hat{H}_\xi G(\boldsymbol{x};\boldsymbol{x}') = \alpha \delta(\rho - \rho') \delta(\xi - \xi'). \qquad (19)$$

Equation 19 is satisfied by the function $G(\boldsymbol{x};\boldsymbol{x}')$ for both cases of boundary conditions of the original differential problem. In addition, for the case of the Dirichlet boundary conditions, $G(\boldsymbol{x};\boldsymbol{x}')$ satisfies

$$G(\boldsymbol{x};1,\xi') = 0 \qquad (20)$$

$$G(\boldsymbol{x};\rho',\xi'+\epsilon) = 0 \qquad \text{(causality)}. \qquad (21)$$

Using Eqs. 19, 20 and 21 and applying $\lim_{\epsilon \to 0}$ in Eq. 18 gives

$$c(\boldsymbol{x}) = \langle G(\boldsymbol{x};\rho',0), c^0(\rho) \rangle - \frac{1}{\alpha} \int_0^\xi d\xi' G_\rho(\boldsymbol{x};1,\xi') c_w(\xi') + \frac{1}{\alpha} \int_0^\xi d\xi' \langle G(\boldsymbol{x};\boldsymbol{x}'), Q(\boldsymbol{x}') \rangle. \qquad (22)$$

Equation 22 is the formal solution in integral equation form to the differential problems described in the second section for the case of Dirichlet boundary conditions at the wall. Equation 22 contains three terms that correspond to three physical aspects of the original problem. The first term is the contribution to the temperature or concentration profile due to the input conditions. The second term contains the effect of the wall temperature $\theta_w(\xi)$ or concentration $c_w(\xi)$, and the third term displays the effect of the bulk homogeneous heat or chemical reaction sources. The function $G(\boldsymbol{x};\boldsymbol{x}')$ in Eq. 22 will be properly identified in a following section.

For the case of von Neumann boundary conditions, Eq. 20 must be replaced with

$$G_\rho(\boldsymbol{x};1,\xi) = 0 \qquad (23)$$

to give

$$c(\boldsymbol{x}) = \langle G(\boldsymbol{x};\rho',0), c^0(\rho) \rangle + \frac{1}{\alpha} \int_0^\xi d\xi' G(\boldsymbol{x};1,\xi') \Omega_w(\xi') + \frac{1}{\alpha} \int_0^\xi d\xi' \langle G(\boldsymbol{x};\boldsymbol{x}'), Q(\boldsymbol{x}') \rangle, \qquad (24)$$

where, as before, the boundary conditions of the original physical problem have been used and the operator $\lim_{\epsilon \to 0}(\cdot)$ has been applied. Equation 24 is the integral solution to the original differential problem given by Eq. 4 and the boundary-entrance conditions given by Eqs. 7a and 7b with von Neumann boundary condition at the wall, that is, Eqs. 8a and 8b. Equations 22 and 24 are, in general, implicit equations since the reaction sources $Q(\boldsymbol{x}')$ and $\Omega_w(\rho')$ can be functions of the concentration variables $c(\rho,\xi)$ that, in turn, are the solutions to the mass transfer problems. The first term in Eq. 24, as for the Dirichlet problem, Eq. 22, is the contribution due to the entrance conditions, $c^0(\rho)$. The second term corresponds to the mass flux at the wall, and the third term, similarly to the Dirichlet problem, is the contribution arising from the volumetric source, $Q(\boldsymbol{x})$. The form of the function $G(\boldsymbol{x};\boldsymbol{x}')$ is related to that of Eq. 22 and it will be specified in a following section.

Identification of the associate eigenvalue problems

The procedure for identifying the eigenvalue problems is considered in this section. A new test function, $\phi_n(\rho)$, will be used in an integration of Eq. 16 to yield

$$\langle \phi_n(\rho'), H_\xi u(\boldsymbol{x}') \rangle = \langle \phi_n(\rho'), Q(\boldsymbol{x}') \rangle, \qquad (25)$$

where $u(\boldsymbol{x})$ is the solution to the differential problem that satisfies the homogeneous boundary conditions, $\langle , \rangle$ is the inner product defined in Eq. 15, and H_ξ the operation given in Eq. 16. An integration by parts performed on Eq. 25 leads to

$$\langle u(x'),L\phi_n(\rho')\rangle - \alpha\frac{\partial}{\partial\xi}\langle\phi_n(\rho'),u(x')\rangle + \rho[\phi_n(\rho)u_\rho(x) - \phi_{n\rho}(\rho)u(x)]_0^1 = \langle\phi_n(\rho'),Q(x')\rangle. \quad (26)$$

The Stürm–Liouville problem associated with the radial diffusion operator L is

$$L\phi_n(\rho) = \lambda_n^2 R(\rho)\phi_n(\rho) \quad (27)$$

$$\rho[\phi_n(\rho)u_\rho(x) - \phi_{n\rho}(\rho)u(x)]|_{\rho=0} = 0 \quad (28a)$$

$$\rho[\phi_n(\rho)u_\rho(x) - \phi_{n\rho}(\rho)u(x)]|_{\rho=1} = 0 \quad (28b)$$

For the homogeneous Dirichlet boundary conditions of the original problem, Eqs. 28a and 28b reduce to

$$\phi_n(1) = 0 \quad (29a)$$

$$\phi_n(0) = 0 \quad (29b)$$

For the homogeneous von Neumann case Eqs. 28a and 28b reduce to

$$\phi_{n\rho}(1) = 0 \quad (29c)$$

$$\phi_{n\rho}(0) = 0. \quad (29d)$$

Using Eq. 27, Eqs. 28a and 28b yield

$$b_{n\xi}(\xi) + \left(\frac{\lambda_n^2}{\alpha}\right)b_n(\xi) = \left(-\frac{1}{\alpha}\right)I_n(\xi), \quad (30)$$

where

$$b_n(\xi) \equiv \langle\phi_n(\rho'),u(x')\rangle \quad (31)$$

$$I_n(\xi) \equiv \langle\phi_n(\rho'),Q(x')\rangle. \quad (32)$$

Equation 30 requires an entrance condition that may be derived from the original problem as

$$b_n(0) = \langle\phi_n(\rho'),\theta^0(\rho')\rangle. \quad (33)$$

Now, the general solution to Eq. 30 is given by

$$b_n(\xi) = b_n(0)\exp\left(-\frac{\lambda_n^2}{\alpha}\xi\right) + \int_0^\xi d\xi' \exp\left[-\frac{\lambda_n^2}{\alpha}(\xi-\xi')\right]\frac{I_n(\xi')}{\alpha}. \quad (34)$$

This equation will play an important role in determining the solution to the differential problem with homogeneous boundary conditions (see the following section). Equation 34 requires calculation of $\{\lambda_n\}$ and $\{\phi_n(\rho)\}$. These eigenvalues and eigenfunctions can be obtained by solving the eigenvalue problems given by Eqs. 27, Eqs. 29a and 29b or 29c and 29d.

From Eq. 15 it is a straightforward task to obtain the normalization factor for the function $\phi_n(\rho)$

$$A_n^2 \equiv \|\phi_n(\rho)\|^2 = \int_0^1 d\rho' R(\rho')\phi_n^2(\rho'). \quad (35)$$

Note, for convenience all subsequent references to $\phi_n(\rho)$ will refer to the normalized eigenfunctions.

Spectral (Mercer) expansion of the Green's function

The solution to the differential heat- and mass-transfer problems with homogeneous boundary conditions can be derived by using the superposition principle of linear equations to obtain

$$c(x) = u(x) = \sum_n b_n(\xi)\phi_n(\rho), \quad (36)$$

where $b_n(\xi)$ is the set of functions given by Eq. 34 and the $\phi_n(\rho)$ are the normalized eigenfunctions obtained from the eigenvalue problems identified in the previous section. After using Eqs. 34 in Eq. 36, it is possible to write

$$u(x) = \left\langle\left[\sum_n^\infty \exp\left(\frac{-\lambda_n^2}{\alpha}\xi\right)\phi_n(\rho')\phi_n(\rho)\right]c^0(\rho')\right\rangle + \frac{1}{\alpha}\int_0^\xi d\xi'\left\langle\left[\sum_n^\infty \exp\left[\frac{-\lambda_n^2}{\alpha}(\xi-\xi')\right]\phi_n(\rho)\phi_n(\rho')\right],Q(x')\right\rangle, \quad (37)$$

where the summation and integration operations have been interchanged. Equation 37 is the formal integral solution to the differential problem with homogeneous boundary conditions. For the case of Dirichlet boundary conditions it is identical to Eq. 22 with $c_w(\xi) = 0$, and for the case of von Neumann it is identical to Eq. 24 with $\Omega_w(\xi) = 0$. By comparing these equations term by term, the Green's function can be found to be

$$G(x;x') = \sum_n^\infty \exp\left[\frac{-\lambda_n^2}{\alpha}(\xi-\xi')\right]\phi_n(\rho')\phi_n(\rho)\hat{\theta}(\xi-\xi'), \quad (38)$$

where $\hat{\theta}(\xi-\xi')$ is the Heaviside (step) function. From Eq. 38

$$G(x;\rho',0) = \sum_n^\infty \exp\left(\frac{-\lambda_n^2}{\alpha}\xi\right)\phi_n(\rho)\phi_n(\rho')\hat{\theta}(\xi-\xi'), \quad (39)$$

$$\left.\frac{\partial G}{\partial\rho}\right|_{\rho'=1} \equiv G_\rho(x;1,\xi') = \sum_n^\infty \exp\left[\frac{-\lambda_n^2}{\alpha}(\xi-\xi')\right]\phi_n(\rho)\phi_{n\rho}(1)\hat{\theta}(\xi-\xi'), \quad (40)$$

and

$$G(x;1,\xi') = \sum_{n}^{\infty} \exp\left[\frac{-\lambda_n^2}{\alpha}(\xi - \xi')\right]\phi_n(\rho)\phi_n(1)\hat{\theta}(\xi - \xi'). \quad (41)$$

With these results, the formal integral solution of the differential problems with Dirichlet and von Neumann boundary conditions at the wall is now complete. It is important to recognize that Eqs. 38 and 41 are formal expressions for the Green's function for any boundary conditions. The evaluation of λ_n and $\phi_n(\rho)$ must be considered properly for the specific cases of Dirichlet or von Neumann types of boundary conditions. The solution strategy for these problems is addressed below.

Solution to the Eigenvalue Problems

The solution to the eigenvalue problems for both types of boundary conditions (i.e., Dirichlet and von Neumann) will be discussed in this section. Both eigenvalue problems can be proved to be self-adjoint (Weinberger, 1965). Moreover, the operator L, defined by the differential operation L after Eq. 11 and boundary conditions given by Eqs. 29a and 29b is a self-adjoint operator in the Hilbert spaces H. Self-adjoint properties to the operator determine that the set $\{\phi_n(\rho)\}$ is a complete set, that the set $\{\lambda_n\}$ belongs to the real numbers, and $\forall\, \lambda_n \neq 0$ the eigenvalues will be positive (Friedman, 1956).

Dirichlet boundary condition

The eigenvalue problem for this case is given by Eq. 27 along with Eqs. 29a and 29b. The solution to Eq. 27 can be related to the hypergeometric confluent equation (Lawerier, 1950, 1951; Abramowitz and Stegun, 1965) by using the transformations

$$a_n \equiv \frac{1}{2} - \frac{\lambda_n}{4}; \qquad b_n \equiv 1, \forall n; \qquad y \equiv \lambda_n \rho^2 \quad (42)$$

for fixed n. The solution to Eq. 27 is now given by

$$\phi_n(\rho) = \exp\left[-\frac{\lambda_n^2 \rho^2}{2}\right]\Psi_n(y), \quad (43)$$

where

$$\Psi_n(z) \equiv c_1 M(a_n,1,y) + c_2 U(a_n,1,y). \quad (44)$$

The functions $M(\cdot)$ and $U(\cdot)$ are the fundamental solutions of the hypergeometric confluent equation (Kummer's equation) and c_1, c_2 are two integration constants. Because $U(\cdot)$ has a singularity at the origin ($y = 0$) (Ederlye, 1953), boundary condition 29b requires that $c_2 \equiv 0$. Therefore Eq. 44 reduces to

$$\Psi_n(y) = c_1 M(a_n,1,y). \quad (45)$$

The set of functions $\{\phi_n(\rho)\}$ with $\Psi_n(y)$ given by Eq. 45 is known as Poiseuille's set of functions since it gives solutions to heat/mass transfer problems of the Hagen–Poiseuille type (Lawerier, 1951). Using these Poiseuille's functions and boundary conditions 29a and 29b, the following characteristic equation is found:

$$M(a_n,1,\lambda_n) = 0, \quad (46a)$$

where $M(a_n,1,\lambda_n)$ is given by the general series

$$M(a_n,b_n,y) = 1 + \sum_{0}^{\infty} \frac{(a_n)_i y^i}{(b_n)_i i!}, \quad (46b)$$

where

$$(a_n)_i = (a_n)(a_n+1)(a_n+2)\cdots(a_n+i-1)$$

$$(b_n)_i = (b_n)(b_n+1)(b_n+2)\cdots(b_n+i-1).$$

The eigenvalues of the operator L that correspond to the Dirichlet boundary conditions are the roots of the characteristic Eq. 46a. These roots, $\{\lambda_n\}$, can be obtained by solving Eq. 46a with standard computational techniques. Table 1 shows the first ten eigenvalues for the Dirichlet case. These calculations have been made with approximately one hundred terms in the hypergeometric series of the Poiseuille functions. Table 1 also shows eigenvalues published in the literature (Jacob, 1949; Villadsen and Michelson, 1978) in the first column. The values of this column compare very well with the ones that were calculated using the methodology of this article. The advantages of the approach discussed here are that it is relatively easy from a computational point of view to produce a large number of eigenvalues within a desired accuracy. Figure 1a shows the first five normalized eigenfunctions $\phi_n(\rho)$ and Figure 1b shows the next five ($n = 5$–10) normalized eigenfunctions corresponding to the eigenvalues λ_n given in Table 1. An interesting characteristic to be observed is that the oscillatory behavior of the functions $\phi_n(\rho)$ with respect to the radial variable ρ increases one branch per eigenvalue. This behavior implies that the function $\phi_n(\rho)$ shows only one branch in the domain $0 \leq \rho \leq 1$ for $n = 1$; two branches, for $n = 2$, three branches for $n = 3$, and so on. The nature of this behavior is useful for numerical simulations in regarding of points that must be used (in the variable ρ) to be able to capture the shape of the function $\phi_n(\rho)$. Also, the effect of the boundary condition is projected from the position $\rho = 0$ up to a position $\rho \cong 0.2$ for the first

Table 1. First Ten Eigenvalues for the Dirichlet Boundary Condition Case

n	Literature Values[a]	This Work
1	2.7044	2.70436
2	6.6790	6.67903
3	10.6734	10.67107
4	14.6711	14.67107
5	18.6699	18.66987
6	22.6691	22.66916
7	26.6681	26.66866
8	30.6683	30.66832
9	34.6681	34.66807
10	38.679	38.66788

[a]Data from Jacob (1949), and Villadsen and Michelson (1978).

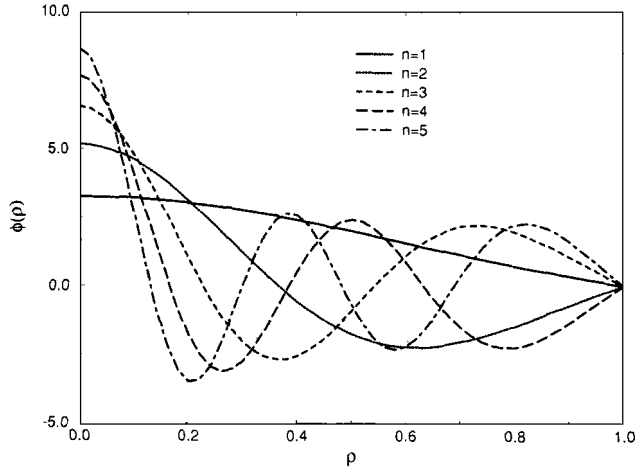

(a)

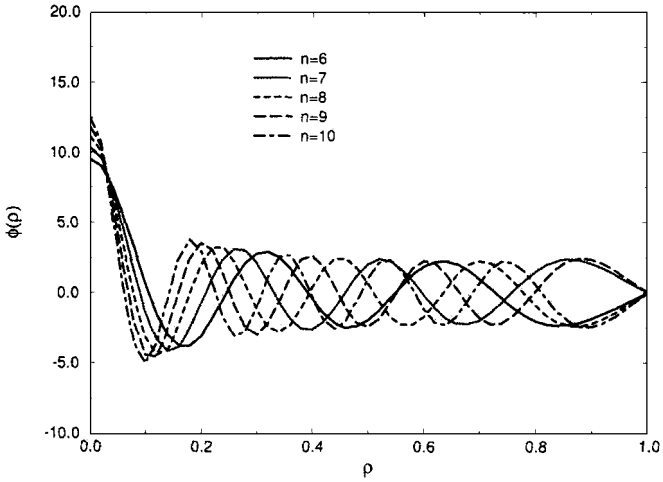

(b)

Figure 1. (a) First five normalized eigenfunctions, $\phi_n(\rho)$ for the case of Dirichlet boundary conditions case; (b) normalized eigenfunctions for eigenvalues λ_n from $n=5$ to $n=10$ for the Dirichlet boundary condition case.

few eigenfunctions. In this region only one branch of the eigenfunction is observed for the first five eigenfunctions. The effect of this boundary condition is less powerful when the value of n increases. For example, for $n = 10$, the first branch of the eigenfunction ends around $\rho = 0.1$. At the other end, $\rho = 1$, the last branch of the first few eigenfunctions starts around $\rho = 0.8$, and this value becomes closer to $\rho = 0.9$ when the value of n increases. All of the eigenfunctions meet at $\rho = 1$ at the value $\phi_n(1) = 0$, as required by the boundary condition of the original differential problem.

von Neumann boundary condition

The eigenvalue problem for the von Neumann case is given by Eq. 27 coupled with the boundary conditions Eq. 29c and Eq. 29d. As in the Dirichlet case, this problem is also self-adjoint. Furthermore, the operator L defined with the differential operator Eq. 11 and the boundary conditions Eq. 29c and Eq. 29d is a positive definite operator under the inner product 15 in the function space H defined previously. These properties assure that the set $\{\phi_n(\rho)\}$ is a complete set of eigenfunctions and that $\{\lambda_n\} \epsilon R \forall n$. Furthermore, any $\lambda_n \neq 0$ is a positive real number. The functions $\phi_n(\rho)$ can be computed in an analogous fashion to that for the Dirichlet problem. The formal solution for $\Psi_n(z)$ is also given by Eq. 44; however, the integration constants must be calculated by using Eq. 29c and Eq. 29d. After performing the necessary algebra

$$\left[\exp\left(-\frac{\lambda_n^2}{2}\right) M(a_n, 1, \lambda_n \rho^2)\right]_\rho = 0, \qquad (47a)$$

where the subscript indicates differentiation with respect to the radial coordinate, ρ. This equation also admits the zero eigenvalue. The complete solution to Eq. 47a was obtained by Arce et al. (1988), and the first 20 eigenvalues are given in Table 2. Also, an asymptotic formula for $n \rightarrow$ large was proposed as the solution of the characteristic Eq. 47. The equation is given by

$$\lambda_n \sim 4\left(n + \frac{1}{3}\right), n \rightarrow \text{large} \qquad (47b)$$

and the results yielded by Eq. 47b are included in Table 2. As n increases, the roots to Eq. 47a produced by Eq. 47b become very close to the values of λ computed using numerical routines (Arce et al., 1988).

As in the case of Dirichlet boundary conditions, the computation of the eigenfunctions, $\phi_n(\rho)$ are performed by using Eq. 43, where the values of the first twenty λ_n are given in Table 2. Figure 2a shows the first five normalized eigenfunctions $\phi_n(\rho)$ computed by using the values of λ_n given in Table 2. The next five ($n = 5$–10) eigenfunctions are shown in Fig-

Table 2. First 20 Eigenvalues for the von Neumann Boundary Condition Case and Comparisons with the Eigenvalues Produced by Asymptotic Eq. 47b

n	Literature Values	Computed (λ^c)	Asymptotic (λ^a)	$A_n^2 \times 10^2$
1	5.0675	5.06750	4.33 (1/3)	4.7534
2	9.1576	9.15760	9.0 (1/3)	2.6933
3	13.1972	13.17922	13.0 (1/3)	1.8808
4	17.2202	17.22023	17.0 (1/3)	1.4452
5	21.2355	21.23551	21.0 (1/3)	1.1737
6	25.2465	25.24653	25.0 (1/3)	0.9889
7	29.2550	29.25490	29.0 (1/3)	0.8533
8	33.2616	33.26524	33.0 (1/3)	0.7508
9	37.2669	37.26690	37.0 (1/3)	0.6705
10	41.2715	41.27138	41.0 (1/3)	0.6058
11	45.2753	45.27518	45.0 (1/3)	0.55254
12	49.2785	49.27845	49.0 (1/3)	0.50805
13	53.2813	53.28129	53.0 (1/3)	0.47037
14	57.2839	57.28380	57.0 (1/3)	0.43815
15	61.2861	61.28603	61.0 (1/3)	0.41045
16	65.2880	65.28801	65.0 (1/3)	0.38672
17	69.2898	69.28980	69.0 (1/3)	0.36711
18	73.2918	73.29141	73.0 (1/3)	0.35421
19	77.2932	77.29282	77.0 (1/3)	0.34617
20	81.2945	81.29395	81.0 (1/3)	0.28240

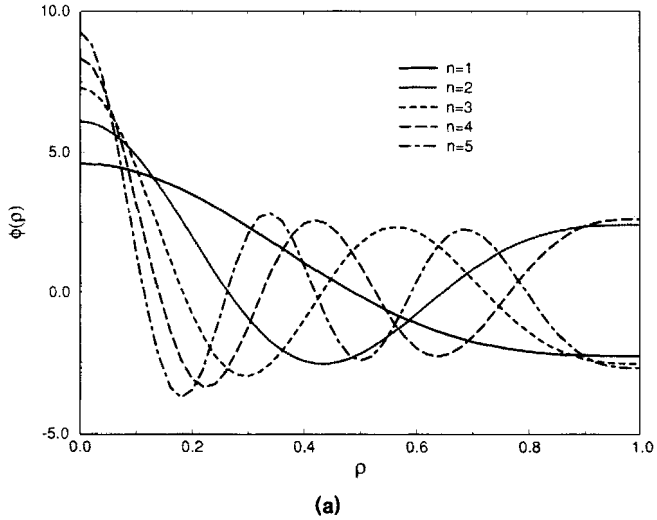

(a)

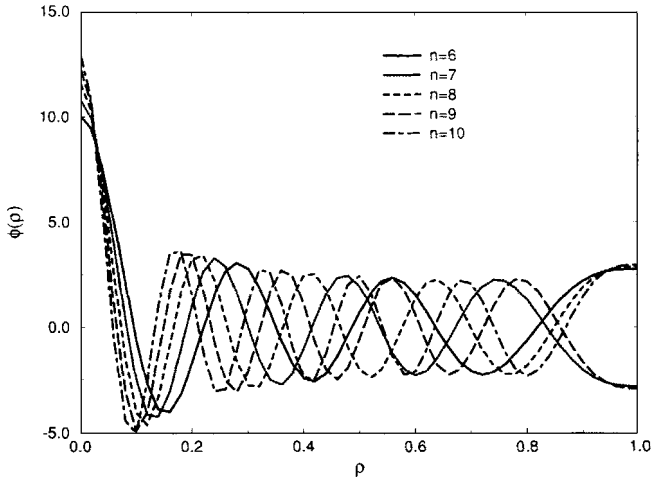

(b)

Figure 2. (a) First five normalized eigenfunctions, $\phi_n(\rho)$ for the von Neumann boundary condition case; (b) normalized eigenfunctions for eigenvalues λ_n from $n=5$ to $n=10$ for the von Neumann boundary condition case.

ure 2b. The oscillatory behavior of these eigenfunctions is similar to that described previously for the case of the Dirichlet boundary conditions. The first 10 eigenfunctions are evenly split around the point zero at the wall position $\rho = 1$ and all of them satisfy the boundary conditions of $\phi_n(1) = 0$ as required by the original differential problem.

The procedure used in this article leads to an eigenvalue problem that is completely independent of all kinetic parameters of the problem and offers a straightforward method that yields large numbers of eigenvalues and eigenfunctions with minimal computational effort. This characteristic of the method will be very useful in the illustrative computations since eigenvalue and eigenfunctions of the Stürm–Liouville problems associated with the operator $\boldsymbol{L}$ can be computed once for all types of chemical reactions kinetics involved in the various cases of the reactor. This saves considerable time in the computations required to obtain the radial concentration profiles.

Alternate Solution for the Dirichlet Problem

Equation 22 gives the formal integral solution to the differential problem with Dirichlet boundary conditions. This integral requires the Green's function given by Eq. 38 and derivatives given by Eq. 40. It is well known that integral equations featuring Green's functions as kernels must be used carefully when computing the actual solution since they contain singularities at the boundaries (Kellog, 1953). Solutions for the function $\theta_w(\xi)$ at the boundary contain Fourier series that, in general, converge very slowly (Haberman, 1987). An alternative approach for improving the integral solution is to derive a solution that features a particular solution $\theta_p(x)$ that satisfies the boundary conditions and a modified transport equation. Thus, the general solution will be given by

$$\theta(x) = \theta_h(x) + \theta_p(x), \tag{48}$$

where the function $\theta_h(x)$ satisfies the problem with homogeneous boundary conditions. The function $\theta(x)$ will satisfy a transport equation that features a modified general source term given by

$$\hat{Q}(x) = [\psi(x) - 2R(\rho)\hat{\psi}(x) + Q(x)]\frac{1}{(1-\rho^2)}, \tag{49}$$

where the functions $\psi(x)$ and $\hat{\psi}(x)$ are given by

$$\psi(x) \equiv \frac{\partial \theta_p}{\partial \xi}(x) \tag{50}$$

$$\hat{\psi}(x) \equiv \frac{\partial}{\partial \rho}\left[\rho \frac{\partial \theta_p}{\partial \rho}(x)\right], \tag{51}$$

respectively. The function $Q(x)$ is the original nondimensional source term given after Eq. 4. For the particular solution $\theta_p(x)$ it is possible to find a family of functions of the type

$$\theta_p^{(n)} = \rho^n \theta_w(\xi), \qquad n \geq 2. \tag{52}$$

It is immediately recognized through Eq. 52 that $\theta_p^{(n)}$ satisfies the nonhomogeneous boundary conditions at $\rho = 1$ and that

$$\left.\frac{\partial \theta_p^{(n)}}{\partial \rho}\right|_{\rho=0} = n\rho^{(n-1)}\theta_w(\xi) = 0 \tag{53}$$

for any $n \geq 2$. Using the functions given by Eq. 52 and Eq. 53, it is a straightforward task to show

$$\psi(x) = \rho^n \frac{\partial \theta_w(\xi)}{\partial \xi} \tag{54}$$

and

$$\hat{\psi}(x) = \theta_w(\xi)[n\rho^{(n-1)} + n\rho(n-1)\rho^{(n-2)}]. \tag{55a}$$

For the particular case of $n = 2$, this equation reduces to the simpler form

$$\hat{\psi}(x) = 2\rho\,\theta_w(\xi). \tag{55b}$$

The function 55b and Eq. 52 define the alternate solution for the Dirichlet problem. The $\theta_h(x)$ function is given by the integral solution Eq. 22, which now satisfies the problem with homogeneous boundary conditions.

Computational Aspects

The integral equation solutions of the problems discussed in this article can be written in a generic form as

$$w(x) = w(x_0) + \int_{x'} dx' K(x;x') f[w(x')], \tag{56}$$

where $K(x;x')$ is the kernel of the integral equation which, for the different cases discussed in the previous sections, features the Green's functions given by Eq. 38 with properties given by Eq. 39 or Eq. 40. The function $f[w(x)]$ is given by the homogeneous source terms. Equation 56 is known as a special case of the so-called nonlinear Hammerstein–Volterra type of integral equations (Goldberg, 1979) and, in general, it must be solved by numerical techniques. Several computational schemes may be used (Goldberg, 1979) including successive iterations, collocation methods, and finite elements. If the method of successive iterations is applied, then from Eq. 56 one obtains

$$w_{k+1}(x) = w_k(x_0) + \int_x dx' K(x;x') f[w_k(x')], \tag{57}$$

where $w_k(x)$ is the concentration (or temperature) profile corresponding to the iteration k. For the case of $K(x;x')$ bounded, the convergence criterion for Eq. 57 is given by Lipzchitz (Coddington and Levinson, 1955) for the function $f[w(x)]$

$$|f[w_{k+1}(x)] - f[w_k(x)]| \le L|w_{k+1}(x) - w_k(x)|, \tag{58}$$

where L is the so-called Lipzchitz constant that coincides with the Damköhler number for the case of homogeneous reactions with $n = 1$ (first-order reactions). When condition 58 is satisfied, the uniqueness condition for the solutions $w(x)$ is also satisfied. Equation 58 is satisfied by a wide variety of source terms, as will be seen in forthcoming studies. Equation 57 is solved numerically for several mass transfer with chemical reactions cases in a section below by the Piccard's method (the successive iteration method). The technique is fast and reliable and it is easy to implement the steps of the computational algorithm.

In solving the integral equation there are three types of errors that must be properly bounded. The first error arises in truncating the series that define the Green's functions given, for example, by Eq. 38. To compute this series, a finite number of terms must be found, and therefore, an error is produced in the process. For a given norm, this error may be indicated as $\|K(x;x') - K_n(x;x')\| \equiv E_1$, where n is the numbers of terms used in the series of the kernel, K. The number n usually depends on the number of eigenvalues used in computing the solution to the integral equation (Goldberg, 1979). Another error corresponds to the evaluation of the integral by numerical techniques, and is given by $\|\int_x dx' g(x') - \sum_1^L g(x_j)h_j\| \equiv E_2$. This error is a function of the method used to compute the integration (i.e., Simpson, quadrature, etc.) indicated earlier. Finally, there is also an error in determining the solution that will satisfy the integral equation itself that can be denoted by $\|w_{k+1}(x) - w_k(x)\| \equiv E_3$. The total error is therefore given as $E_T = E_1 + E_2 + E_3$. It is important in calculations to monitor a relationship such as $E_1 \ll E_2 \ll E_3$ in order to have meaningful results for the solution $w(x)$ of the integral equation.

The integral–spectral approach developed in the previous sections will be applied to several cases with reactions at the wall, homogeneous (bulk) reactions, and simultaneous catalyzed wall and bulk reactions. The kinetics used in the calculation will be mainly focused on nonlinear functions such as the power-law and the Laugmuir–Hinshelwood types.

Homogeneous (Bulk) Reactions

This section discusses the application of the technique developed earlier to the homogeneous tubular reactor with bulk reactions that have rate expressions given by power law expressions or Michaelis–Menten or Langmuir–Hinshelwood forms. The methodology is general and could be applied to other reaction rate forms. It will be given in this section. The homogeneous tubular reactor with laminar flow has applications in several industrial processes (Trombetta and Happel, 1966; Tan and Hsu, 1971) and in laboratory analysis to extract information from reacting systems such as transport parameters and kinetic rate functions (Lupa and Dranoff, 1966; Villameaux, 1981; Subramanian and Berhe, 1972; Dang, 1983).

Several different techniques have been used to solve the mathematical models resulting from the class of problems considered here. The methods include, for example, finite differences (Cleland and Whilhelm, 1956), solutions based on eigenfunction expressions (Hsu, 1965; Schecter and Wissler, 1960), and the methods of moments (Aris, 1980). In general, the cases addressed in these previous analyses are limited to first-order reactions (Lawerier, 1959; Nigam, 1982), simplified models for photoreactions (Schechter and Wissler, 1960), and some simple cases of polymerization reactions (Ray and Laurence, 1977). Due to the simplifying nature of the assumptions made in the model formulation, some semianalytical expressions have been obtained (Ogren, 1975; Nigam, 1982). In this section the general integral solution derived in the previous sections of this article will be applied to several cases of the laminar flow tubular reactor. The focus is on nonlinear kinetics and, in particular, power-law forms and Michaelis–Menten or Langmuir–Hinshelwood types of rate law expressions. In the first case, global reactions of a generalized nth order have a kinetic equation of the following type:

$$R(\hat{c}) = \nu k \hat{c}^n(x), \tag{59}$$

where the integer $n(n \ge 0)$ may take the usual values 0, 1, 2, and 3, and it also can take fractional values in the interval

$0 < n < 1$. The nondimensional form of Eq. 59 is

$$\hat{\Omega}(x) = -D_a c^n(x), \tag{60}$$

where $\nu = -1$ and D_a is the Damköhler number of the first kind (Carberry, 1977; Cunningham and Lombardi, 1978) defined as $kR^2/D(c^0)^{1-n}$.

Another example of homogeneous reactions considered in this section is the enzymatic type, which can be described by a Michaelis–Menten form. The mathematical equation corresponding to this kinetics is given by

$$R(\hat{c}) = \frac{\nu k\hat{c}(x)}{\hat{K} + \hat{c}(x)}. \tag{61}$$

The nondimensional version of this equation is given by

$$\hat{\Omega}(x) = \frac{-D_a c(x)}{K + c(x)}. \tag{62}$$

As before, D_a is the Damköhler number of first kind and K is a nondimensional constant.

The reactor model for the case of homogeneous (bulk) reactions is given by Eq. 4 in nondimensional concentration variables and parameters with the constant $\alpha = 2PeGe$. For this reactor analysis ξ is in the domain $0 < \xi < 1$. The boundary condition at the center of the reactor, $\rho = 0$, is given by the symmetry condition, Eq. 8a, and at the wall, $\rho = 1$, the boundary condition is given by Eq. 8b with $\Omega_w \equiv 0$ since in this case no reaction is assumed at the external wall. At the inlet of the reactor, the condition is given by Eq. 9. The function $c_e(\rho)$ may take any of the nonuniform distributions, but for illustration, a constant (uniform) distribution will be assumed. The effect of other distributions are presented elsewhere (Arce et al., 1992).

The formal solution to the reactor model described earlier is given by Eq. 24 with $\Omega_w(\xi) = 0$ and the function $Q(x')$ replaced by the nondimensional kinetic rate function given by Eq. 60 or Eq. 62:

$$c(x) = \langle G(x;\rho',0),c^0\rangle + \frac{1}{\alpha}\int_0^{\xi} d\xi' \langle G(x;x'),\Omega(x')\rangle, \tag{63}$$

where $\Omega(x) \equiv \hat{\Omega}(x')/(1-\rho^2)$ as given after Eq. 4. The first term on the righthand side is the contribution of the inlet condition to the concentration profile, and this will be evaluated for the particular case of $c^0 = 1$. The second term on the right-hand side of Eq. 63 is the contribution from the homogeneous chemical reaction, $\Omega(x)$. For the case of a constant inlet concentration:

$$\langle G(x;\rho',0)c^0\rangle = \int_0^1 d\rho' R(\rho') G(x;\rho',0)c^0$$

$$= c^0 \sum_{n=0}^{\infty} \gamma_n \phi_n(\rho) e^{-\beta_n \xi}, \tag{64a}$$

where $\beta_n \equiv \lambda_n^2/\alpha$ and the factor γ_n has been identified as (Lee and Aris, 1977)

$$\gamma_n \equiv \int_0^1 d\rho' R(\rho') \phi_n(\rho'), \tag{65}$$

where γ_n can be related to the boundary condition at the wall, $\rho = 1$, by using the eigenvalue problem identified previously. The result is (see Appendix 1)

$$\gamma_n = -\frac{\phi_{n\rho}(\rho = 1)}{\lambda_n^2}, \tag{66}$$

where the subscript ρ indicates differentiation with respect to ρ. This equation implies (see Corollary I of Appendix 1) that the values of $\gamma_n = 0$, $\forall n \neq 0$. For the case of $n = 0$, ($\lambda_0 = 0$); however, γ_n can be calculated by using its mathematical definition, Eq. 65, to give $\gamma_0 = 1/2$. This value satisfies the relation $\gamma_0\phi_0 = 1$ according to the definition of the normalization constants. These interesting properties of the constant γ_n imply that the value of the term corresponding to the inlet conditions is one provided that the nondimensional concentration is given by $c^0 = 1$. Therefore, the general solution for the homogeneous tubular reactor with a uniform inlet distribution is given by the equation

$$c(x) = 1 + \frac{1}{\alpha}\int_0^{\xi} d\xi' \langle G(x;x'),\Omega(x')\rangle. \tag{67}$$

Figure 3a shows radial averaged conversion profiles, that is, $\chi(\xi)$, for first-order kinetics with different values of the Damköhler number, D_a. The profiles were computed using Eq. 67 with a successive approximation technique as discussed in the previous section. All the calculations were made for $\alpha = 100$, using the zero eigenvalue and the 20 eigenvalues of Table 2, and with two hundred terms in the series of Poiseuille functions given by Eq. 45. The figure shows that a value of $D_a = 10$ yields a conversion profile that is practically linear and that reaches a maximum conversion less than 1% (0.75%) at the outlet of the reactor. If the Damköhler number is changed to a value of $D_a = 500$, the conversion rises very sharply in the first half of the reactor, reaching a value of 87.83% at the axial position $\xi = 0.50$. The maximum conversion is 98.23% at the outlet of the reactor. This value drops to 79.29% when the $D_a = 100$ and to a value of 57.5% when $D_a = 50$.

Figure 3b shows the effect of the order of the reaction on the conversion profiles $\chi(\xi)$. These calculations were performed for $\alpha = 100$ and $D_a = 50$ and using the same number of eigenvalues and terms in the Poiseuille functions as before. The figure shows the exponential increase in the conversion profile that is typical of parabolic differential models where the largest conversion is obtained for the zero-order kinetics and the smallest for the case of $n = 2$. All the conversion profiles meet at the origin at the inlet of the reactor, and they reach maximal values at the outlet. The maximum conversion varies between $\chi(1) = 0.461$ (for $n = 2$) and $\chi(1) = 0.796$ (for $n = 0$). The outlet conversion of the reactor decreases by about 33.5% when the order goes from $n = 0$ to $n = 2$, and by about 11.41% when the order is changed from $n = 1$ to $n = 2$. The difference in conversion at the axial position $\xi = 0.5$ is 17.42% when the zero-order reaction is compared with the second-order reaction.

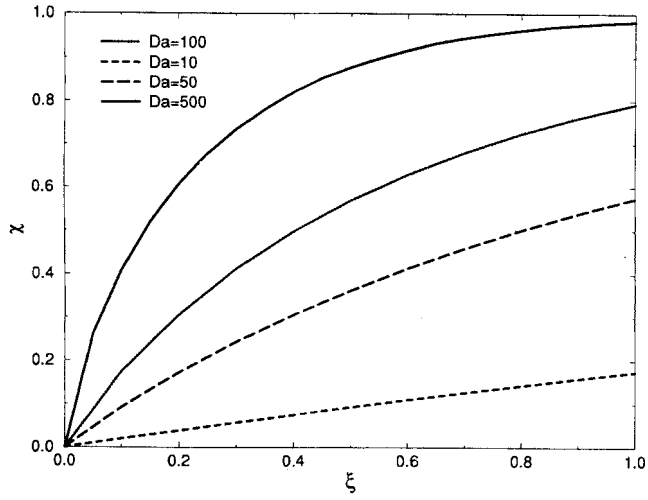

(a)

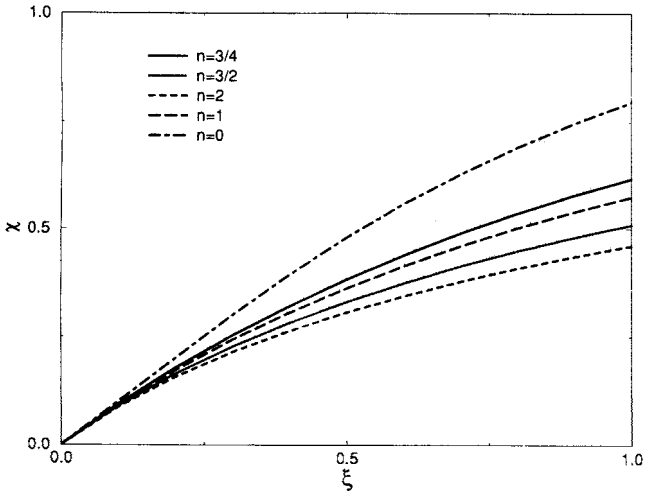

(b)

Figure 3. Conversion profiles for the case of homogeneous reactions with power-law kinetics.

(a) Effect of the Damköhler number for axial conversion profiles for first-order case. (b) Effect of the order of reaction on the axial conversion profiles.

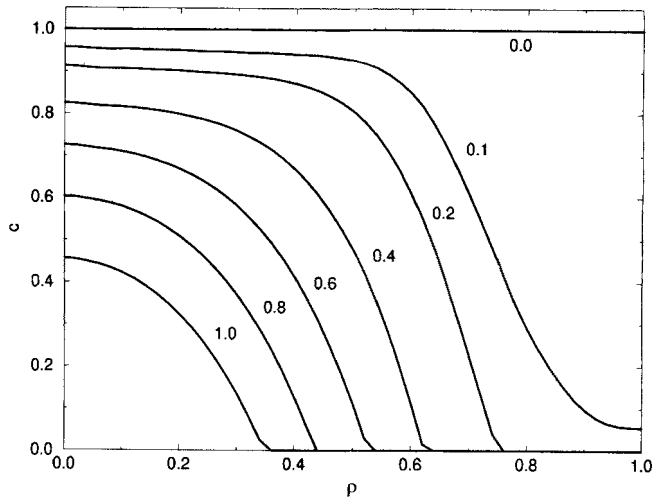

Figure 4. Radial conversion profiles for different axial positions.

Figure 4 shows radial concentration profiles for the case of first-order reaction with $\alpha = 20$ and $D_a = 20$. The figure shows profiles for various axial positions of the reactor from $\xi = 0$ to $\xi = 1$ (outlet). The calculations show that the profiles satisfy the symmetry boundary condition at the center ($\rho = 0$) and the no flux condition at the wall, $\rho = 1$ (see, for example, $\xi = 0.1$). Also, values beyond $\xi = 0.2$ show that the reactant concentration has been depleted to a zero value within the reactor for a range of the radial position. This range is located near the wall since those radial positions have a larger residence time than those closer to the center due to the parabolic nature of the velocity profile.

Effects of the type of kinetic expression on the conversion profiles are shown in Figures 5a, 5b and 5c for the values of $\alpha = 100$ and $D_a = 50$. Three different kinetic expressions (variations of the Langmuir–Hinshelwood type) have been used in the calculations performed for these figures. Figure 5a shows a parametric analysis with respect to constant K for the kinetics of the form $D_a c/(K + c^{1/2})^2$. For a value of $K = 0.2$, the outlet conversion of the reactor is 32.52%; when the value of K is increased to $K = 1$, the outlet conversion drops to 11.88%. When the value of K is maintained at $K = 1$, but the kinetic expression is changed to $D_a c/(K + c)$, the outlet conversion is 40.45% (Figure 5b), which shows an important effect with respect to reactant conversion in the reactor. Figure 5c shows the effect of the order n of the reaction when kinetics of the type $D_a c^n/(K + c)$ are used. The value of $n = 1$ with $K = 0.5$ yields an outlet conversion of 52.41% (Figure 5b). When the value of n is increased to $n = 1.5$ and $n = 2$ as observed before, the conversion drops to 45.81% and 41.14% at the outlet of the reactor, respectively.

Wall-Catalyzed Reactions

This section is devoted to the application of the integral formulation to the analysis of wall-catalyzed reactors. These reactors, which also have been called "active-wall" reactors (see Farina, 1979), have applications in a variety of chemical engineering processes. For example, catalytic wall reactors have been used in catalytic converters for automobiles (Young and Finlayson, 1976; Lee and Aris, 1972), a certain class of methane converters (Froment and Bischoff, 1990), biotechnological applications (Horvath and Engasser, 1973), and in the food processing industry. Active wall reactors are also used in polymer processes where laminar flow is necessary due to viscosity limitations (Tadmor and Gogos, 1979). More recently there has been an increasing interest in modeling and experimental work in membrane reactors. This type of reactor can also be considered as an example of "active wall" reactors; however, in certain cases the transport inside the membrane must be taken into account. There are two alternatives for considering transport in the membrane. One possibility is to use an effectiveness factor to modify the reaction rate at the internal wall to account for the transport limitations inside the membrane. Another alternative would be to consider both domains (the fluid domain and the membrane domain) simultaneously. In this investigation, a lumped membrane system,

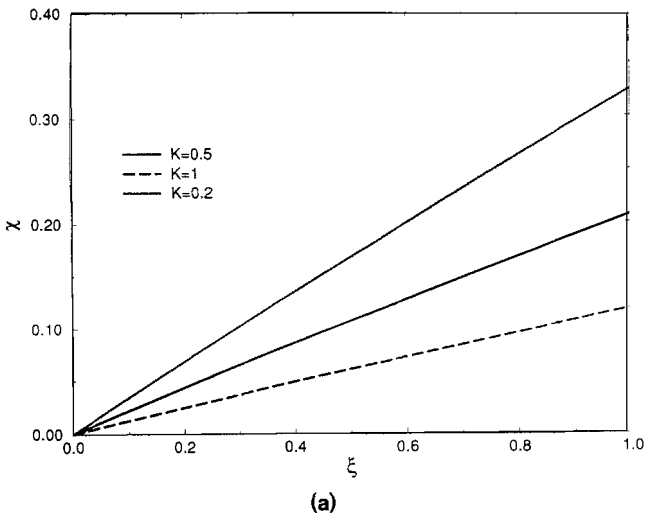

(a)

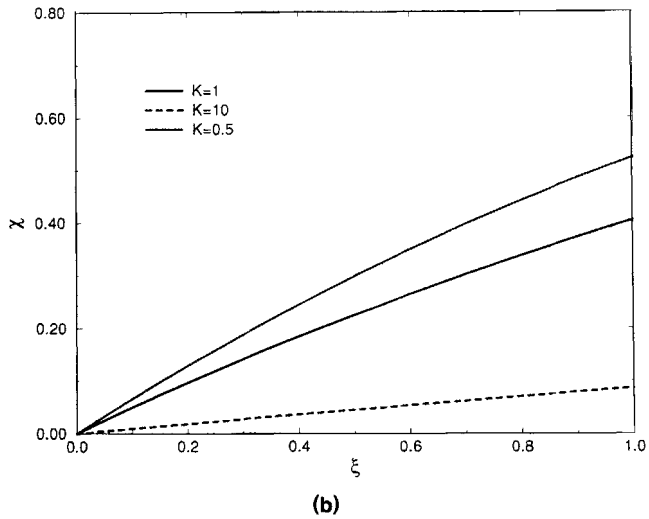

(b)

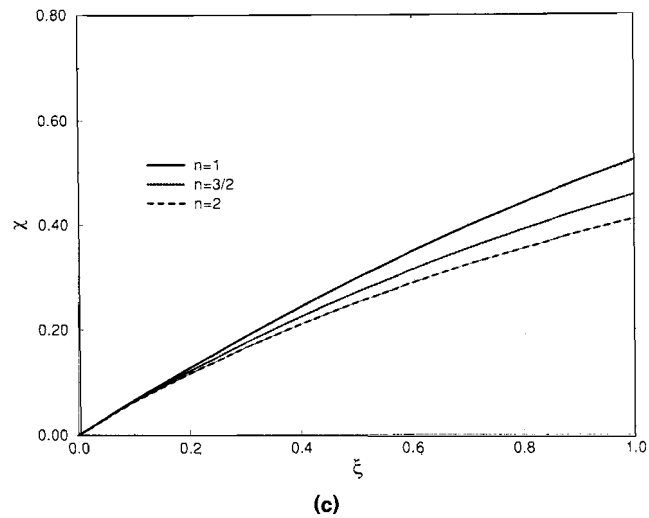

(c)

Figure 5. Conversion profiles for the case of homogeneous reaction with different kinetic types.

(a) Axial conversion profiles for different K values for a kinetics of the type $D_a c/(K + c^{1/2})^2$. (b) Effect of the K values on the axial conversion profiles for the case of $D_a/(K + c)$. (c) Effect of the order of reaction on the axial conversion profiles kinetics given by $D_a c^n/(K + c)$.

that is, with an effectiveness factor of unitary value, will be considered. Work is in progress to study cases where the transport limitation inside the membrane must be included (Arce and Locke, 1994).

Physical systems displaying convective–diffusive transport and reactions on the surfaces (i.e., boundary of the physical domain) have been studied in the past. Earlier contributions go back to Chambre (1956), who developed an analysis to account for the hydrodynamics of the boundary layer and the catalyzed reaction at the wall. Chambre and Acrivos (1956) and Acrivos and Chambre (1957) discussed the formulation of laminar boundary layer models with surface reactions under isothermal conditions. The solution of these problems is valid for a limited class of rate functions. Furthermore, by approximating the fluid velocity profile near the catalytic surface, they derived integral equations that allow the calculation of concentration gradients at the wall. The effect of homogeneous reactions on boundary layer flows has also been studied (Leal, 1992), and the effect of diffusional transport on the falsification of activation energy and reaction order was investigated by Rosner (1963). These investigations are all for the case of external flow systems (flows over flat surfaces) and, in general, they focus on relatively simple reaction rate functions. Internal flows such as, between two parallel plates with zero-order surface-catalyzed chemical reactions have been investigated by Rosner (1966). This author also presented exact and approximate solutions for laminar and turbulent boundary layer flows along flat plates (i.e., external flows). Surface-catalyzed reactions have been discussed by Katz (1959) who used a Laplace transform approach and focused mainly on the kinetic analysis of the problem.

The general molar species continuity equation for the case of wall reactions is given by Eq. 4 with nondimensional variables and parameters and with $Q(c, \theta) = 0$. The boundary conditions for the radial coordinate of the reactor are given by symmetry Eq. 8a at the center of the reactor and by Eq. 8b at the wall. The function $\Omega_w[c_w, \theta_w]$ will be assumed to be given by $\Omega_w[c_w]$ since isothermal conditions are considered. Different types of reaction expressions may be considered since the solution methodology can handle any type of kinetic equations. Langmuir–Hinshelwood kinetics will be considered in this section and are given by

$$R[\hat{c}_w(\xi)] = \frac{\nu k(T)\hat{c}_w(\xi)}{[\hat{K}(T) + \hat{c}_w(\xi)]}, \tag{68}$$

where $k(T)$ is the kinetic constant, $\hat{K}(T)$ the equilibrium (adsorption–desorption) constant, and $c_w(\xi)$ the concentration of the reactant at the wall of the reactor. Equation 68 can be nondimensionalized to yield

$$\Omega_w[c_w(\xi)] = \frac{-D_{aw}c_w(\xi)}{[K + c_w(\xi)]}. \tag{69}$$

This equation has two important limiting forms: the zero-order reaction limit is achieved when $c_w(\xi) \gg K$, and the first-order case will be obtained when $c_w(\xi) \ll K$. The latter case usually implies a weak adsorption of the reactant species

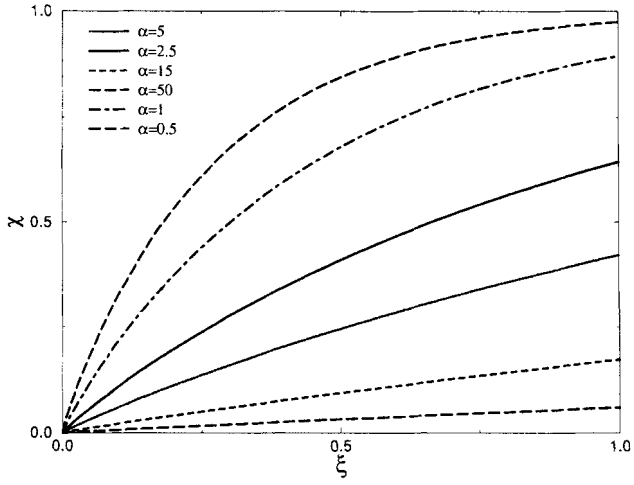

(a)

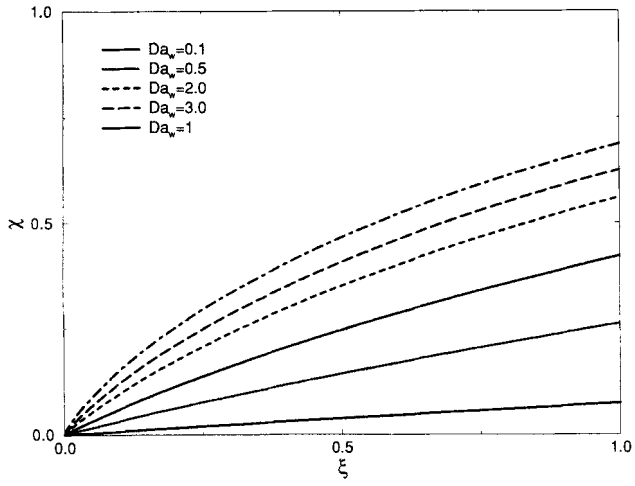

(b)

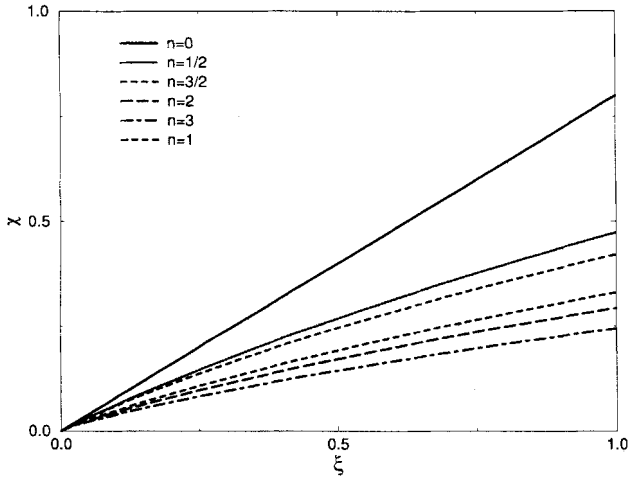

(c)

Figure 6. Axial conversion profiles for the case of *n*th-order wall-catalyzed reaction.

(a) Effect of the residence time for first-order reaction. (b) Effect of the wall Damköhler number for first-order reaction. (c) Effect of the order of the bulk reaction.

on the catalytic surface. Variations of this kinetics will also be used in the illustrative examples studied in a section below.

The integral equation that must be solved coupled with the various kinetics described earlier can be obtained as a particular case of Eq. 24. The last term of this equation becomes zero since $Q(x) = 0$. Also, the first term of this equation is one as shown in the previous section for the case of uniform inlet distributions. This equation is a nonlinear Volterra integral equation of the second kind. The equation requires iteration only at $\rho = 1$ (for $c_w(\xi)$) as opposed to $0 < \rho < 1$ for the differential problem. Thus a two-dimensional (2-D) problem has been effectively reduced to a 1-D problem. Also, in implementing the computational approach of the section titled "Computational Aspects" in the resulting equation for the wall-catalyzed reactions case, the Gibbs phenomena have been corrected by following an approach discussed in Arce and Locke (1994). This procedure requires closed Fourier expansions that have been derived in Appendix 1 of this article.

Figure 6a, 6b, and 6c show a parametric study of the behavior of the reactor when a nth-order catalyzed reaction is taking place at the wall. Figure 6a shows the effect of the residence time of the reactor on the radial averaged conversion profiles through the parameter α for a wide range of values. An increase in the value of the parameter α ($\alpha = 2PeGe$) implies that the averaged residence time decreases, and therefore the conversion level also decreases. For example, in Figure 6a, a value of $\alpha = 0.5$ yields a conversion level at the output of the reactor of 97.6%, while a value of $\alpha = 5$, which is an increase of ten times with respect to the previous value of α produces a conversion of only 42.1% at the outlet of the reactor. A value of $\alpha = 50$ reduces the conversion of the reactor outlet to a value of 6.07%. Also, a value of α larger than $\alpha = 5$ yields an almost linear behavior of the conversion profile with respect to the axial coordinate of the reactor, ξ. On the other hand, a value of, for example, $\alpha = 0.5$ produces a very nonlinear increase in the conversion within the first half of the reactor. This particular behavior suggests that an axial gradient in the catalyst activity may be useful to effectively utilize the whole length of the reactor in an optimal way (Arce et al., 1992).

Figure 6b shows the effect of a variation in the Damköhler number at the wall, D_{aw}, on the conversion profiles for $\alpha = 5$. A value of $D_{aw} = 0.1$ yields an output conversion of 7.4%, while when the D_a is increased ten times, the conversion goes to a value of 42.1% at the reactor outlet. Figure 6c shows the results of the conversion, $\chi(\xi)$, as the order of the reaction is changed for fixed values of $D_a = 1$ and $\alpha = 5$. The results indicate that a zero-order reaction yields an output conversion of 80% and that this value drops to 47% when the order is changed to $n = 0.5$. A value of $n = 3$ produces a conversion of only 24% at the reactor outlet.

Figure 7a shows computations for the case of a Langmuir–Hinshelwood reaction at the wall of the reactor, given by $D_{aw}c/(K + c)$. The calculations were performed using $\alpha = 5$ and $D_{aw} = 1$. The value of K was varied within the range between $K = 0$ (zero-order reaction) and $K = 10$. The values of the conversion of the reactor at the outlet ranges between 80% ($K = 0$) and 67% ($K = 10$). The results show that when the constant K's doubled from $K = 0.5$ to $K = 1$, the outlet conversion drops from 39% to 30%, indicating that

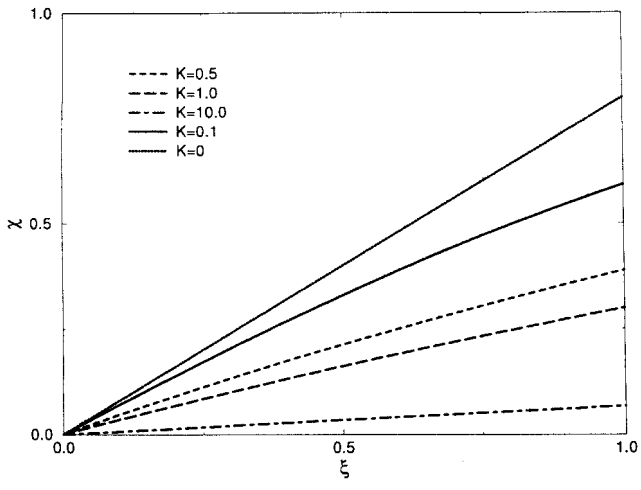

(a)

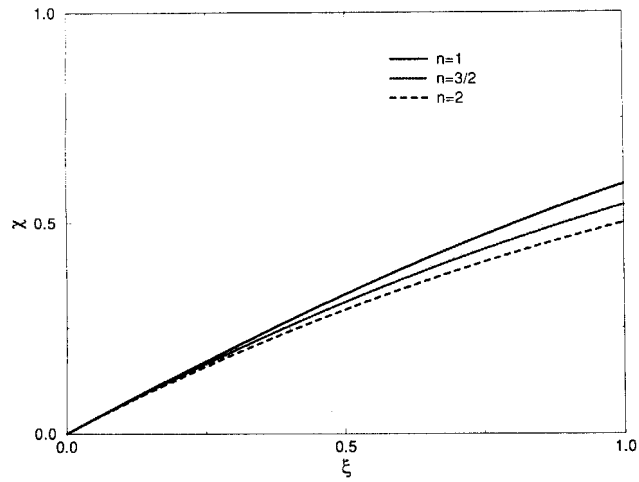

(b)

Figure 7. Axial conversion profiles for the case a Langmuir–Hinshelwood reaction at the wall given by $D_{aw}c^n/(K+c)$.

(a) Effect of the parameter K for $n=1$. (b) Effect of the order of the wall reaction.

for the conditions of the calculation a high accuracy in K value may not be of great importance.

Figure 7b shows the effect of the order of the wall reaction, n, when a kinetics of the type $D_a c^n/(K+c)$ is used at the wall of the reactor. For the value of $\alpha = 5$ and $D_{aw} = 1$. The most important variation is obtained when the order is changed from $n=0$ to $n=1$; the differences in the outlet conversion for values of n between $n=1$ and $n=3$ are located within the range of 59.2% and 50%.

Simultaneous Surface (Wall) and Homogeneous Reactions

Simultaneous surface (wall) and homogeneous (bulk) reactions are important in a number of industrial processes. Some of these include photochemical reactions in, for example, photochlorination, photochemical desulfination, and photooxidation (Braun et al., 1991), photocatalytic reactions of importance in water and air pollution control (Serpone and Pelizzetti, 1989), and hydrocarbon pyrolysis in petrochemical systems (Badger, 1967). Many petrochemical and pyrolysis reaction systems must be modeled by taking into account the wall termination steps. In some cases, the effect of these (wall tube) reactions have an important effect on the overall behavior of a homogeneous reactor and they cannot be ignored (Froment, 1971). In general, the study of these homogeneous–heterogeneous systems has focused on chemical reactions with simplified kinetics (Solomon and Hudson, 1966; Dang, 1983). In this section we present a solution scheme for this type of simultaneous (bulk and wall) reactions with the possibility of having nonlinear kinetics expressions of any type. Examples may include power law kinetics forms and/or Langmuir–Hinshelwood kinetics. The solution strategy follows the case of surface catalyzed reactions and homogeneous (bulk) reactions that were discussed previously. Furthermore, analysis for the simpler cases of zero-order reactions are also presented. Some numerical illustrations for key cases are included.

Within the framework of the analysis discussed in this article, and from the mathematical point of view, the case of simultaneous surface (wall) and homogeneous (bulk) reactions is more complicated since it requires the use of two of the three terms involved in the general solution given by Eq. 24 and it requires iteration over both spatial variables:

$$c(\boldsymbol{x}) = \langle G(\boldsymbol{x};\rho',0), c^0(\rho')\rangle + \left(\frac{1}{\alpha}\right)\int_0^{\xi} d\xi' G(\boldsymbol{x};1,\xi')\Omega_w[c_w(\xi)] + \left(\frac{1}{\alpha}\right)\int_0^{\xi} d\xi' \langle G(\boldsymbol{x};\boldsymbol{x}'), \Omega[c(\boldsymbol{x}')]\rangle. \quad (70)$$

This equation can be reduced further for the case of uniform inlet concentrations, that is, $c^0(\rho') = 1$. For this situation, the input term (the first term of the right-hand side) reduces to unity. If, for example, Langmuir–Hinshelwood kinetics is used for the wall reactions (Eq. 69) and power law kinetics, for the homogeneous reactions (Eq. 60), then the solution for the case under analysis is given by

$$c(\boldsymbol{x}) = 1 - \left(\frac{D_{aw}}{\alpha}\right)\int_0^{\xi} d\xi' G(\boldsymbol{x};1,\xi')\frac{c_w(\xi')}{K + c_w(\xi')} - \left(\frac{D_a}{\alpha}\right)\int_0^{\xi} d\xi' \left\langle G(\boldsymbol{x};\boldsymbol{x}'), \left[\frac{c^n(\boldsymbol{x}')}{(1-\rho'^2)}\right]\right\rangle. \quad (71)$$

The first term on the right-hand side in Eq. 71 is the effect of the inlet distribution (a constant term), the second term is the contribution of the wall-catalyzed reaction, and the third term is the effect of the bulk reaction. The solution to Eq. 71 has been obtained following the procedure described in the previous section and the section titled "Computational Aspects."

Parametric calculations varying the adsorption–desorption constant K (Figure 8a), the Damköhler number at the wall D_{aw} (Figure 8b), the bulk Damköhler number (Figure 8c), and the order of the catalyzed reaction in the bulk, n (Figure 8d), were performed for the case of $\alpha = 16$. For the case of Figure 8a the values of D_a and D_{aw} are such as $D_a = D_{aw} = 1$.

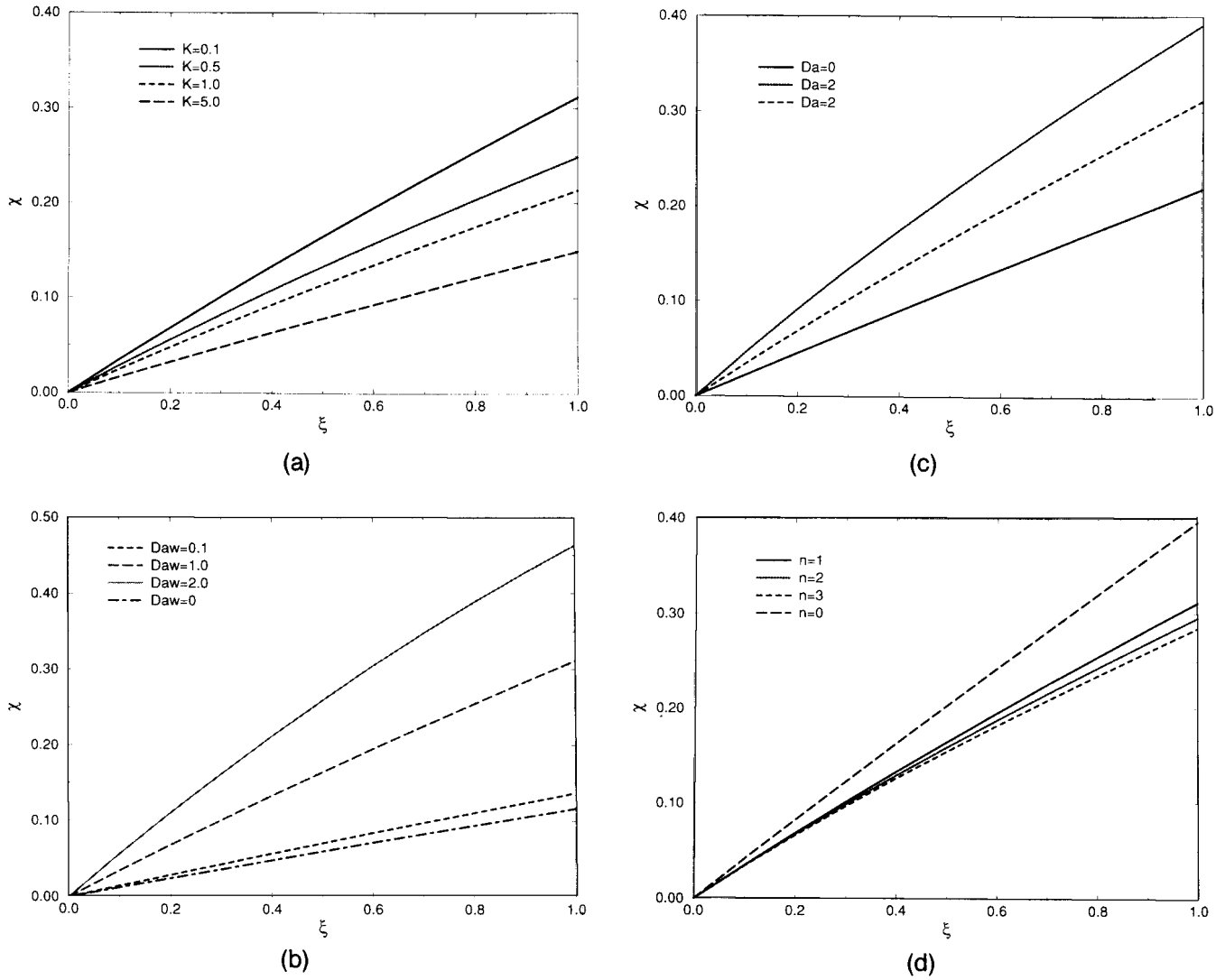

Figure 8. Axial conversion profile for the case of first-order bulk reaction and a Langmuir–Hinshelwood reaction at the wall given by $D_{aw}c/(K+c)$.

(a) Effect of the parameter K. (b) Effect of the wall Damköhler number. (c) Effect of the bulk Damköhler number. (d) Effect of the bulk reaction order.

The conversion profiles for the reactor show a slight exponential behavior for the different values of K and the output conversion of the reactor is located within the range of 14.91% (for $K = 5.0$) and 31.17 (for $K = 0.1$). A value of $K = 0.1$, $\alpha = 16$, and $D_a = 1$ were used in the computations that are shown in Figure 8b. This figure shows the effect of the reaction at the wall (of a Langmuir–Hinshelwood type) when the bulk reaction follows a first-order kinetics. The overall conversion reaches a value of only 11.6% when the wall reaction is not present ($D_{aw} = 0$), but it increases up to a value of 46.33% when the value of $D_{aw} = 2$. When D_{aw} is increased by ten times (from $D_{aw} = 0.1$ to $D_{aw} = 1$) the conversion at the outlet of the reactor goes from a value of 13.68% to one of 31.17%, which indicates a change of approximately 127.85% in the output conversion of the reactor. This value although important, represents a relatively small change in the output conversion, that is, 2.28 times vs. the magnitude of the change in the Damköhler mentioned previously.

Figure 8c represents the effect of the bulk reaction on the catalytic reaction at the wall. The wall reaction follows a Langmuir–Hinshelwood kinetics of the type $D_{aw}c/(K+c)$ with $K = 0.1$, $D_{aw} = 1$, and $\alpha = 16$. This case may be viewed as the effect of a side (bulk) reaction on the overall conversion in the system when the reaction of interest occurs at the wall of the reactor. For example, when the bulk reaction is not present ($D_a = 0$) the output conversion is only 21.87%; however, this value increases to 31.1% when $D_a = 1$ and to 39.11% when $D_a = 2$. These calculations suggest that an important part of the reactant is being converted to nondesirable products in the reactor even for relatively small values of the Damköhler number of the bulk reaction. Figure 8d shows the effect of the change of the order of the reaction in the bulk when a Langmuir–Hinshelwood kinetics occurs at the wall of the reactor. As before the most important change in the output conversion is obtained when the order n goes from $n = 0$ to $n = 1$. Higher values of n yield only relatively small changes in the output conversion of the reactor. The zero-order reaction case is treated in Appendix 2.

Summary and Concluding Remarks

An integral–spectral approach for laminar flow systems with homogeneous (in the bulk of the fluid) and heterogeneous (at the wall) sources has been obtained. The solution is valid for heat or mass transfer processes without sources such as chemical reactions or with generalized source functions. The solution is, in the general case, formal since it is an integral equation. For heat or mass sources that do not depend upon temperature or concentration (i.e., linear problems), an analytical solution can be obtained. The general solution obtained in this article reduces to analytical expressions known in the literature for simpler cases such as the Graetz problem (Graetz, 1883, 1885; Newman, 1973). The integral equation features a kernel given by the Green's function, which is expressed in terms of the eigenvalues and eigenfunctions of the associated Stürm–Liouville problem. This problem is solved completely in terms of known analytical functions (Poiseuille functions), which result from a combination of exponential and Kummer functions (Lawerier, 1951). These functions provide a very efficient way to solve the characteristic equation and to complete the eigenfunctions of the problem. The approach is fast, direct, and reliable. Moreover, asymptotic forms can be obtained for the computation of a large number of eigenvalues in cases where they are needed. The Green's function has mathematical features common to all laminar flow situations and, interestingly, it is independent of factors, such as the sources, that are specific to each problem. This is a very useful aspect in order to avoid repetitive computational effort when treating different cases, as was illustrated in the different applications considered in this article.

The reason that the Green's function shows the characteristics mentioned earlier is that the eigenvalue problem arises from the linear transport operator for the laminar convection and the radial diffusion without including the source terms. This decoupling of sources and transport is the essential characteristic of the Green's function approach followed in this analysis that gives rise to an improved computational strategy. The results of the present effort are useful for developing computational schemes that are economical in time and have a fast convergence rate. The analysis reported here is focused on axial convective and diffusive (radial) transport without axial dispersive transport or axial conduction; however, the operator framework introduced in this article can be extended to include this case as well as the case of transport in multiphase interactive systems. This will be the subject matter of future contributions.

For the case of catalytic reaction at the wall, nonhomogeneous boundary conditions are observed and therefore the Gibbs phenomena arising from the Fourier expansion must be handled properly in order to yield the correct results. The present analysis has followed a methodology described in Arce and Locke (1994) that can be used to construct efficient computational algorithms to overcome the Gibbs phenomena. The technique is based on closed sums of Fourier expansions of linear problems; however, they can be used for solving problems featuring nonlinear kinetics. The proposed technique is an alternative to the classical Lanczos methodology to smooth the impact of the Gibbs phenomena in Fourier expansions. Although the proposed method has been applied to Poiseuille reacting flows, its validity is more general and it can be extended to other convective–diffusive transport problems. Some of these cases will be the subject matter of future publications.

Acknowledgments

Pedro Arce and Bruce R. Locke have received partial support from special research grants from the Council of Research and Creativity (CRC) of the Florida State University during the period of performing the investigation reported in this article. Portions of this work were presented at the Annual AIChE Meeting at Miami Beach, FL, November 1992 and at St. Louis, MO, November 1993. The early version of the manuscript was typed by Brian Scott, and the final revisions by Heidy Booeshaghi.

Notation

A_n = normalization constant in Hilbert space H
a_n = transformation in Kummer functions
c = nondimension (molar) concentration
c' = molar species concentration
$c_b(\xi)$ = bulk concentration profile
Ge = geometric function
$K(T)$ = adsorption–desorption constant
L = length of tube
$Q(x)$ = nondimensional heat generation, after Eq. 4
r = radial coordinate
R = tube radius
$R(c)$ = reaction rate function
$R_j[C_j]$ = reaction rate of the jth reactant species
$\hat{R}(\rho)$ = weighing function of the inner product of L in H
$x \equiv (\rho, \xi)$ = vector of independent spatial coordinates
$U(\cdot)$ = fundamental solution of Kummer's equation
x = vector of spacial coordinates, dimensional
$y = \lambda_n \rho^2$
z = axial coordinate, dimensional

Subscripts and superscripts

n = number of terms in expansion
i = dummy variable of integration
$\hat{}$ = dimensional variable; dimensional quantity
b = bulk
n = eigenvalue index
n = reaction order

Greek letters

α = coefficient defined in Eq. 2
β = equilibrium coefficient at the wall, Eq. 10
β_n = function of eigenvalue λ_n and α, $= \lambda_n^2/\alpha$
$\chi(\rho, \xi)$ = local reactor conversion, $(c^o - c)/c^o$
$\chi_w(\xi)$ = wall reactor conversion
ν = stoichiometric coefficient
$\hat{\Omega}$ = nondimensional reaction rate, Eq. 2
$\Psi_n(\rho)$ = integral function of Poiseuille function; function of the variable ρ
ρ_m = fluid density

Literature Cited

Abramowitz, M., and I. A. Stegun, *Handbook of Mathematical Functions*, Dover, New York (1695).

Acrivos, A., and P. L. Chambre, "Laminar Boundary Layer Flows with Surface Reactions," *Ind. Eng. Chem.*, **49**(6), 1025 (1957).

Andersen, T., and J. Coull, "Evaluation of Models for Tubular, Laminar Flow Reactors," *AIChE J.*, **16**, 542 (1970).

Arce, P., H. Irazoqui, and A. Cassano, "The Tubular Reactor with Laminar Flow Regime. An Integral Equation Approach: I. Homogeneous Reaction with Arbitrary Kinetics," *Comp. Chem. Eng.*, **12**(11), 1103 (1988).

Arce, P., and B. R. Locke, "Transport and Reaction: An Integral Equation Approach. Mathematical Formulation and Computational Approaches," *Research Trends in Chemical Engineering*, J.

Menon, ed., Vol. 2, p. 89, Council of Scientific Information, India (1994).
Arce, P., H. Irazoqui, and A. Cassano, "An Integral Equation for the Modeling of Laminar Reacting Flow Systems," *Tech. Res. Rep.*, National Council for Scientific Research, CONICET, Argentina (in Spanish) (1983).
Arce, P., B. R. Locke, and I. M. B. Trigatti, "The Hollow Fiber Membrane Reactor: An Integral Equation Approach," paper presented at the AIChE Meeting, Miami Beach, FL (Nov., 1992).
Arce, P., B. R. Locke, and I. M. B. Trigatti, "An Integral-Spectral Approach for Convective-Diffusive Transfer in Tubular Poiseuille Flows with Heat Sources," submitted (1995).
Aris, R., "On the Dispersion of a Solute in a Fluid Flowing Through a Tube," *Proc. Roy. Soc. A*, **235**, 67 (1956).
Aris, R., "Hierarchies of Models in Reactive Systems," *Dynamics and Modelling of Reactive Systems*, W. E. Steward, W. H. Ray, and Ch. C. Conley, eds., Academic Press, New York (1980).
Ayappa, K. G., G. Crapiste, E. A. Davis, H. T. Davis, and T. Gordon, "Microwave Heating: An Evaluation of Power Formulations," *Chem. Eng. Sci.*, **46**, 1005 (1991).
Badger, G. M., "Pyrolysis of Hydrocarbons," *Prog. in Phys. Org. Chemistry*, **1**, 1 (1967).
Barouh, V. A., and M. D. Makhailov, "Homogeneous-Heterogeneous Reactions in a Tubular Reactor," *Int. Comm. Heat Mass Transfer*, **17**, 113 (1990).
Barouh, V. A., and M. D. Makhailov, "One-Dimensional Heat and Mass Diffusion Modelling Software,"*Appl. Math. Modelling*, **13**, 568 (1989).
Beck, J. V., K. D. Cole, A. Haji-Sheikh, and B. Litkouhi, *Heat Conduction Using Green's Functions*, Hemisphere, Philadelphia (1992).
Bird, R. B., W. E. Stewart, and E. N. Lightfoot, *Transport Phenomena*, Wiley, New York (1960).
Braun, A. M., M. T. Maurette, and E. Oliveros, *Photochemical Technology* (Translated by D. F. Ollis and N. Serpone), Wiley, New York (1991).
Brenner, H., "Macrotransport Processes: Brownian Trancers as Stochastic Averagers in Effective-Medium Theories of Heterogeneous Media," *J. Stat. Phys.*, **62**(5/6), 1095 (1991).
Carberry, J. J., *Chemical and Catalytic Reaction Engineering*, McGraw-Hill, New York (1976).
Chambre, P. L., "On Chemical Surface Reactions in Hydrodynamic Flows," *Appl. Sci. Res.*, **A6**, 97 (1956).
Chambre, P. L., and A. Acrivos, "On Chemical Surface Reactions in Laminar Boundary Layer Flow," *J. Appl. Phys.*, **27**(11), 1322 (1956).
Cleland, F., and R. Wilhelm, "Diffusion and Reaction in Viscous-Flow Tubular Reactors," *AIChE J.*, **2**(4), 489 (1956).
Coddington, E. A., and N. Levinson, *Theory of Ordinary Differential Equations*, McGraw-Hill, New York (1955).
Courant, R., and D. Hilbert, *Methods of Mathematical Physics*, Vols. 1 and 2, Wiley Interscience, New York (1953).
Cunningham, R., and J. Lombardi, *Diseño de Reactores Quimicos*, EUDEBA, Buenos Aires, Argentina (in Spanish) (1978).
Dang, D., "Steady-State Mass Transfer with Homogeneous and Heterogenous Reactions," *AIChE J.*, **29**, 19 (1983).
Davis, M. E., and L. T. Watson, "Analysis of a Diffusion-Limited Hollow Fiber Reactor for the Measurement of Effective Substrate Diffusivities," *Biotechnol. Bioeng.*, **27**, 182 (1985).
Delves, L. M., and J. Walsh, *Numerical Solution of Integral Equations*, Clarendon Press, Oxford (1974).
Dranoff, J., "An Eigenvalue Problem Arising in Mass and Heat Transfer Studies," *Math. Comp.*, **xv**, 403 (1961).
Ederlye, M., *Higher Transcendental Functions*, Bateman manuscript Project 1, California Institute of Technology, Pasadena (1953).
Farina, I., "Reactors de Pared Activa," Cuadernos CAMAT #1, Argentinean Committee of Heat and Mass Transfer, CAMAT (in Spanish) (1979).
Friedman, B., *Principles and Techniques of Applied Mathematics*, Wiley, New York (1956).
Froment, G. F., "Some Aspects of the Design of Fixed-Bed Reactors for Hydrocarbon Oxydation," *Period. Polytechnica (Budapest)*, **15**, 219 (1971).
Froment, G., and K. B. Bischoff, *Chemical Reactor Analysis and Design*, 2nd ed., Wiley, New York (1990).
Gidaspow, D., "Green's Functions for Graetz Problems," *AIChE J.*, **17**, 19 (1971).
Giddings, C. J., *Unified Separation Science*, Wiley, New York (1991).
Glasstone, S., *Introduction to Nuclear Reactors*, Wiley, New York (1966).
Golderg, M., *Solution Methods for Integral Equations*, Plenum Press, London (1979).
Golding, J. A., and R. Dussult, "Conversions and Temperature Rises in a Laminar Flow Reactor for the Hydration of Acetic Anhydride," *Can. J. Chem. Eng.*, **56**, 564 (1978).
Gratez, "On the Heat Capacity of Fluids," *Ann. Phys.*, **18**, 79 (1883); "Über die Wärmeleitungsfahigkeit von Flüssigkeitein," *Ann. Phys.*, **25**, 337 (1885).
Grau, R., A. Cassano, and H. Irazoqui, "Mass Transfer Through Permeable Walls: A New Integral Approach for Cylindrical Tubes with Laminar Flow," *Chem. Eng. Comm*, **64**, 47 (1988).
Haberman, *Elementary Applied Partial Differential Equations*, 2nd ed., Prentice-Hall, Englewood Cliffs, NJ (1987).
Horvath, C., and J. M. Engasser, "Pellicular Heterogeneous Catalysts. A Theoretical Study of the Advantages of Shell Structured Immobilized Enzyme Particles," *Ind. Eng. Chem. Fund.*, **12**(2), 229 (1973).
Hsu, C.-J., "Heat Transfer in a Round Tube with Sinusoidal Wall Heat Flux Distribution," *AIChE J.*, **11**, 690 (1965a).
Hsu, C.-J., "A Method of Solution for Mass Transfer with Chemical Reaction under Conditions of Viscous Flow in a Tubular Reactor," *AIChE J.*, **11**, 938 (1965b).
Jacob, M., *Heat Transfer*, Vol. 1, Wiley, New York (1949).
Jaswon, M. A., and G. T. Symm, *Integral Equation Methods in Potential Theory and Elasticity*, Academic Press, New York (1977).
Karilla, S. J., and S. Kim, "Integral Equations of the Second Kind for Stokes Flow: Direct Solution for Physical Variables and Removal of Inherent Accuracy Limitations," *Chem. Eng. Comm.*, **82**, 123 (1989).
Katz, S., "Chemical Reactions Catalyzed on a Tube Wall," *Chem. Eng. Sci.*, **6**, 202 (1959).
Kellog, D. D., *Foundations of Potential Theory*, Dover, New York (1953).
Kim, J., and P. Stroeve, "Mass Transfer in Separation Devices with Reactive Hollow Fibers," *Chem. Eng. Sci.*, **43**(2), 247 (1988).
Kim, S., and S. J. Karilla, *Microhydrodynamics: Principles and Selected Applications*, Butterworths, Stoneham, MA (1991).
Kitano, H., and N. Ise, "Hollow Fiber Enzyme Reactors," *Trends Biotechnol.*, **2**(1), 26 (1984).
Lawerier, H. A., "The Use of Confluent Hypergeometric Functions in Mathematical Physics and the Solution of an Eigenvalue Problem," *Appl. Sci. Res.*, **A2**, 184 (1950).
Lawerier, H. A., "Poiseuille Function," *Appl. Sci. Res.*, **A3**, 58 (1951).
Leal, G. L., "Laminar Flow and Convective Transport Processes (Scaling Principles and Asymptotic Analysis)," Ser. in Chem. Eng., Butterworth-Heinemann, Boston, MA (1992).
Lee, S. T., and R. Aris, "On the Effects of Radiative Transfer in Monoliths," *Chem. Eng. Sci.*, **32**, 827 (1977).
Lin, S., and J. E. Huff, "Polymerization in Tubular Reactors," *AIChE J.*, **17**, 245 (1971).
Lupa, J., and J. Dranoff, "Chemical Reaction on the Wall of an Annular Reactor," *Chem. Eng. Sci.*, **21**, 861 (1966).
Mansour, A. R., A. M. Shehoul, and A. Nusayr, "An Analytical Solution for Diffusion and Reaction in a Laminar Flow Tubular Reactor," *Int. Comm. Heat Mass Transfer*, **16**, 603 (1989).
Newmann, J., *Electrochemical Systems*, Prentice-Hall, Englewood Cliffs, NJ (1973).
Nigam, K. M., "Homogeneous-Heterogeneous Reactions in a Tubular Reactor: An Analytical Solution," *Chem. Eng. J.*, **25**, 147 (1982).
Ogren, P., "Analytical Results for First Order Kinetics in Flow Tube Reactors with Wall Reactions," *J. Phys. Chem.*, **79**, 17 (1975).
Ray, H., and R. L. Laurence, "Polymerization Reaction Engineering," in *Chemical Reactor Theory. A Review*, I. Lapidus and N. R. Amundson, eds., Prentice-Hall, Englewood Cliffs, NJ, p. 562 (1977).
Rosner, D. E., "The Apparent Chemical Kinetics of Surface Reactions in External Flow Systems: Diffusional Falsification of Activation Energy and Reaction Order," *AIChE J.*, **9**(3), 321 (1963).
Rosner, D. E., "Effects of Convective Diffusion on the Apparent Kinetics of Zeroth Order Surface-Catalyzed Chemical Reactions," *Chem. Eng. Sci.*, **21**, 223 (1966).
Rothenberg, R. I., and J. M. Smith, "Heat Transfer and Reaction in Laminar Tube Flow," *AIChE J.*, **12**, 213 (1966).

Schechter, R. S., and E. M. Wissler, "Photochemical Reactions in an Isothermal Laminar-Flow Chemical Reactor," *Appl. Sci. Res.*, **A9**, 334 (1960).
Schilson, R. E., and N. R. Amundson, "Intraparticle Diffusion and Conduction in Porous Catalyst I and II," *Chem. Eng. Sci.*, **13**, 226, 237 (1961).
Serpone, N., and E. Pelizzetti, eds., *Photocatalysis*, Wiley, New York (1989).
Solomon, R. L., and J. L. Hudson, "Diffusion and Reaction in Ideal Multicomponent Systems—I Tubular Reactor Near Equilibrium," *AIChE J.*, **17**(2), 371 (1971).
Stanley, T. J., and J. A. Quinn, "Phase-Transfer Catalysis in a Membrane Reactor," *Chem. Eng. Sci.*, **42**(10), 2313 (1987).
Stewart, W. E., D. F. Marr, T. T. Nam, and A. M. Gola-Galimidi, "Transport Modelling of Packed-Tube Reactors—I. Framework for a Data Based Approach," *Chem. Eng. Sci.*, 2905 (1991).
Subramanian, S., and S. Berhe, "Unsteady Convective Diffusive in Annular Catalytic Reactor," *Chem. Eng. Sci.*, **31**, 1005 (1976).
Tadmor, Z., and C. G. Gogos, *Principles of Polymer Processing*, Wiley, New York (1979).
Tan, C. W., and C. J. Hsu, "Diffusion of Aerosols in Laminar Flow in a Cylindrical Tube," *Aerosol Sci.*, **2**, 117 (1971).
Tanzosh, J., M. Manga, and H. Stone, *Proceedings of Boundary Elements Technologies VII*, C. A. Brebbia and M. S. Ingber, eds., Computational Mechanic Publications, Cambridge, MA, p. 19 (1992).
Taylor, G. I., "Dispersion of Soluble Matter in Solvent Flowing Slowly Through a Tube," *Proc. Roy. Soc., A*, **218**, 44 (1953).
Taylor, G. I., "Conditions Under Which Dispersion of a Solute in a Stream of Solvent can be Used to Measure Molecular Diffusion," *Proc. Roy. Soc., A*, **225**, 473 (1954a).
Taylor, G. I., "Diffusion and Mass Transport in Tubes," *Proc. Phys. Soc., London, B*, **67**, 857 (1954b).
Tereck, Ch., D. S. Kovak, and M. D. LeVan, "Constant Behavior for Adsorption on the Wall of a Cylindrical Channel," *Ind. Chem. Eng. Res.*, **26**, 1222 (1987).
Trombetta, M. L., and J. Happel, "Analysis and Design of Gas Flow Reactors with Applications to Hydrocarbon Pyrolysis," *AIChE J.*, **11**(6), 1041 (1965).
Urtiaga, A., A. Irabien, and P. Stroeve, "Effect of a Variable Solute Distribution Coefficient on Mass Separation in Hollow Fibers," *Ind. Eng. Chem. Res.*, **31**, 1362 (1992).
Villadsen, J., and M. Michelson, *Solution of Differential Equation Models by Polynomial Approximation*, Prentice-Hall, Englewood Cliffs, NJ (1978).
Villermeaux, J., "Diffusion Dans un Reactor Cylindrique," *Int. J. Heat Transfer*, **14**, 1963 (1971).
Weinberger, H. F., *A First Course in Partial Differential Equations*, Wiley, New York (1965).
Young, L., and B. Finlayson, "Mathematical Models of Monolith Catalytic Converter," *AIChE J.*, **22**(2), 331 (1976).
Ziaka, Z. D., T. T. Tsotsis, and R. G. Minet, "Propane Dehydrogenation in a Catalytic Membrane Reactor," AIChE Meeting, St. Louis (Nov. 7–12, 1993).

Appendix 1

1. Given that $\phi_n(\rho)$ is the Poiseuille's function defined by

$$\phi_n(\rho) = e^{-\beta_n \rho^2} M[a_n, 1, \lambda_n \rho^2] \tag{A1}$$

where $M[\cdot]$ is the Kummer function of first kind, and λ_n is the eigenvalue of the radial diffusion operator L defined in the third section, then the integral numbers $\{\gamma_n\}$ defined as

$$\gamma_n \equiv \int_0^1 d\rho' R(\rho') \phi_n(\rho'), \tag{A2}$$

where $R(\rho) = \rho(1-\rho^2)$, have the following values

$$\gamma_n = -\frac{\phi_{n\rho}(\rho = 1)}{\lambda_n^2}, \tag{A3}$$

where the subscript ρ indicates differentiation with respect to ρ.

Corollary. For the case of Neumann boundary conditions, or, alternatively, flux boundary conditions, γ_n have the following two values

$$\gamma_n = 0 \qquad n \geq 1 \tag{A4a}$$

$$\gamma_n = \frac{1}{2} \qquad n = 0. \tag{A4b}$$

To show that Eq. A3 is true, the use of the eigenvalue problem given by Eq. 33 is required. After integrating Eq. 27 once, the following result is obtained

$$[\rho \phi_n'(1)]_0^1 = -\lambda_n^2 \int_0^1 d\rho' R(\rho') \phi_n(\rho') = -\lambda_n^2 \gamma_n \tag{A5}$$

by making use of the fact that $\phi_n'(0) = 0$ is straightforward to conclude that Eq. A3 is true. Equation A4a can be proved by using $\phi_n'(1) = 0$, $\forall_n \geq 1$. For the case of $\lambda_0 = 0$, by using the definition of γ_n Eq. A4b can be shown by using $\phi_0 = 2$ for the normalized zero eigenfunction.

2. Given that $\phi_n(\rho)$ is the Poiseuille function as indicated in section one of this appendix, then the series is identified as

$$\Psi_s(\rho) = \sum_{n=1}^{\infty} \frac{\phi_n(1)\phi_n(\rho)}{\lambda_n^2} \tag{A6}$$

is the Fourier expansion of the following function

$$\Psi_c(\rho) = \rho^2 - \frac{\rho^4}{4} - \frac{7}{24}. \tag{A7}$$

To establish Eq. A7 the zero-order problem will be used; however, since Eq. A7 is the closed form of Eq. A6, there is no dependence of final closed form on the reaction rate. This can be observed through Eq. A6, where the eigenfunctions and eigenvalues are independent of the kinetics. This is a major advantage of the present approach. In order to show that Eq. A7 is true, we must recognize that

$$\lim_{\xi \to \infty} c(\rho, \xi) = c_\infty(\rho, \xi) = 1 - \left(\frac{4D_{aw}}{\alpha}\right)\xi - D_{aw}\Psi_s(\rho). \tag{A8}$$

Equation A8 can be derived by seeking ξ to be far enough from the reactor inlet entrance so the Eq. A7 immediately leads to the result of Eq. A8. Since the function $\Psi_s(\rho)$ is part of the solution $c(\boldsymbol{x})$, according to Eq. A8, it must satisfy the following differential equation

$$\frac{d}{d\rho}\left[\rho \frac{d\Psi_s}{d\rho}\right] = 4R(\rho), \tag{A9}$$

where $R(\rho)$ was previously defined. Also, $\Psi_s(\rho)$ must satisfy the following boundary conditions

$$\Psi'(\rho)|_{\rho=0} = 0, \qquad \Psi'(\rho)|_{\rho=1} = -1. \tag{A10}$$

Equation A9 and Eq. A10 are easily checked by replacing $c_\infty(\rho,\xi)$ in the differential model given earlier (Eq. 4) with $\Omega(c,\theta) \equiv 0$ and Eqs. 8a and 8b. Also, $c_\infty(\rho,\xi)$ will satisfy an integral balance condition rather than the inlet condition at $\xi = 0$. This condition can be derived by applying the averaging operator given by Eq. 23 to the differential model. The result is

$$c_b(\xi) = 1 - \frac{4D_{aw}}{\alpha}\xi, \tag{A11}$$

where the nondimensional zero-order reactions have used boundary conditions at the wall. Equation A11 leads to

$$4\int_0^1 d\rho' R(\rho')c(\rho',\xi) = 1 - \frac{4D_{aw}}{\alpha}\xi. \tag{A12}$$

Now, by replacing $c(\rho,\xi)$ by $c_\infty(\rho,\xi)$ and using Eq. A8, the following result is true

$$\int_0^1 d\rho' R(\rho')\Psi_s(\rho') = 0. \tag{A13}$$

Equation A13 is an integral constant for the function $\Psi_s(\rho)$ that is a direct result of the integral (or average) balance given by Eq. A12. Now, by integrating Eq. A9 twice, the general equation written below is obtained for function $\Psi_s(\rho)$

$$\Psi_s(\rho) = \frac{1}{4}(4\rho^2 - \rho^4) + c_1 \ln \rho + c_2. \tag{A14}$$

The use of the boundary condition at $\rho = 0$ implies that $c_1 = 0$ and the use of Eq. A14 leads to $c_2 = -\frac{7}{24}$. Replacing these values in Eq. A14 implies that

$$\Psi_s(\rho) = \frac{1}{4}(4\rho^2 - \rho^4) - \frac{7}{24}, \tag{A15}$$

which is, in fact, the result given by Eq. A7.

Corollary. The asymptotic solution $c_\infty(\rho,\xi)$ for the zero-order reaction is given by

$$c_\infty(\rho,\xi) = 1 - \left(4\frac{D_{aw}}{\alpha}\right)\xi + D_{aw}\left[\frac{\rho^4}{4} - \rho^2 + \frac{7}{24}\right]. \tag{A16}$$

This equation can be checked by replacing $\Psi_s(\rho)$ given by Eq. A15 in Eq. A8. Equation A16 is valid for the values of parameters D_{aw} and α such as $c_\infty(\rho,\xi) \geq 0$. For example, based on the wall-outlet conversion, the α and D_{aw} must satisfy the relationship

$$D_{aw} = \frac{1}{\left(\frac{4}{\alpha} + \frac{11}{24}\right)} \tag{A17}$$

in order to comply with $c_\infty(\rho,\xi) \geq 0$.

Appendix 2

The differential model for the limiting case of zero-order bulk and wall reactions as given by

$$\alpha\rho(1-\rho^2)\frac{\partial c}{\partial \xi} = \frac{\partial}{\partial \rho}\left(\rho\frac{\partial c}{\partial \rho}\right) - \rho D_a \tag{A18}$$

can be averaged directly using the definition given by Eq. 24

$$c_b \equiv \frac{\int_0^1 R(\rho)c\,d\rho}{\int_0^1 \rho R(\rho)\,d\rho} = 4\int_0^1 R(\rho)c\,d\rho \tag{A19}$$

and the boundary conditions

$$\left.\frac{\partial c}{\partial \rho}\right|_1 = -D_{aw} \qquad \left.\frac{\partial c}{\partial \rho}\right|_0 = 0. \tag{A20}$$

Applying the average operation of Eq. A19 mentioned earlier directly to the differential model Eq. A18 and using boundary conditions A20 gives

$$\frac{\alpha}{4}\frac{dc_b}{d\xi} = -\left[D_{aw} + \frac{D_a}{2}\right] \tag{A21}$$

and therefore

$$c_b = 1 - \frac{4}{\alpha}\left[D_{aw} + \frac{D_a}{2}\right]\xi \tag{A22}$$

and the conversion for a uniform inlet is then given by

$$\chi(\xi) = \frac{4}{\alpha}\left[D_{aw} + \frac{D_a}{2}\right]\xi, \tag{A23}$$

which would be equivalent to that determined by averaging the solutions of the differential model as proposed in the text.

Manuscript received Apr. 18, 1994, and revision received Dec. 27, 1994.